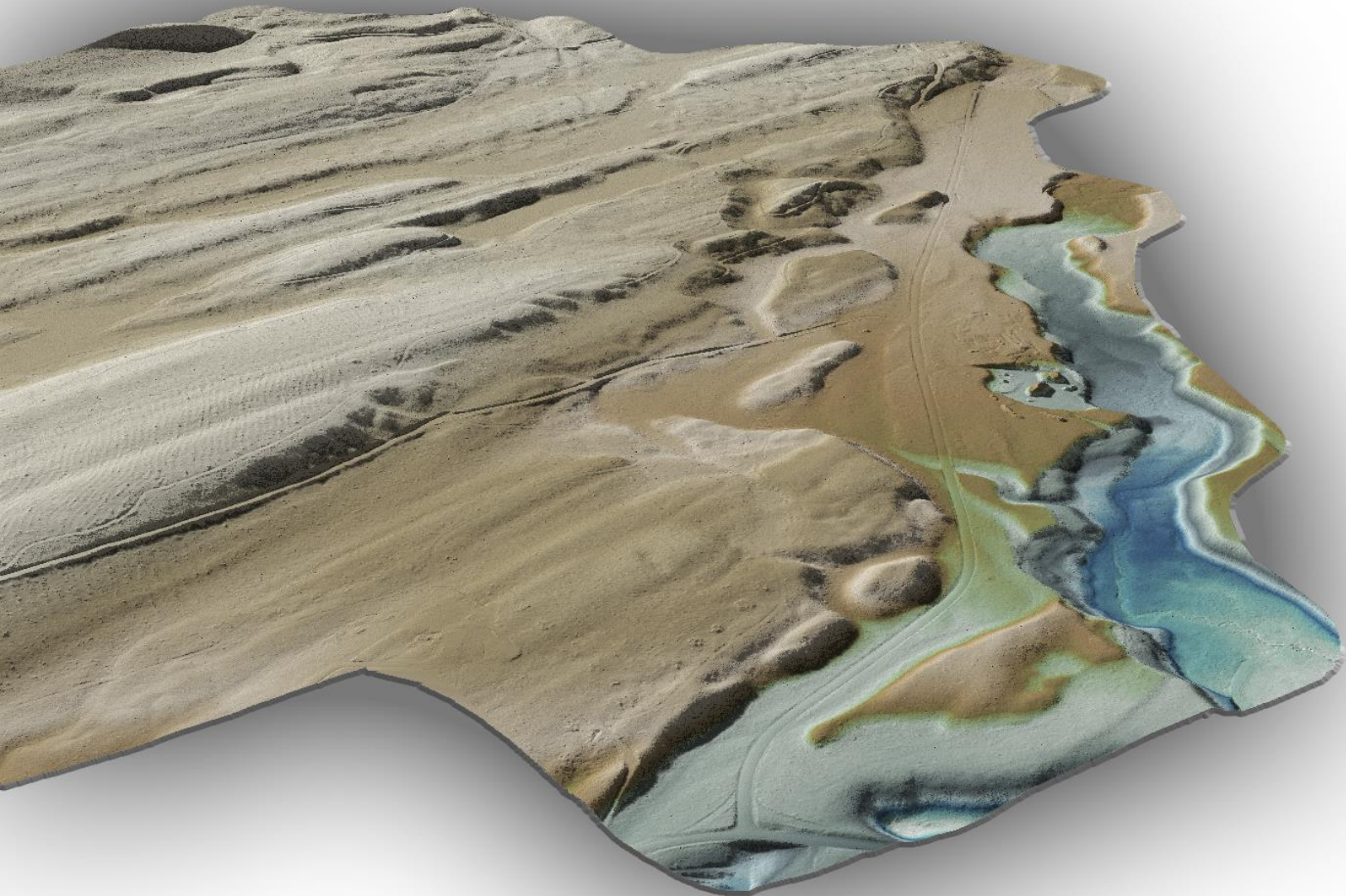




Applied  
Remote Sensing  
and Analysis

November 22, 2013



# Missoula Sites, Montana

## LiDAR Technical Data Report



**Andy Belski**  
River Design Group, Inc.  
5098 Highway 93 South  
Whitefish, MT 59937  
PH: 406-862-4963



WSI Corvallis Office  
517 SW 2nd St., Suite 400  
Corvallis, OR 97333  
PH: 541-752-1204



# TABLE OF CONTENTS

- INTRODUCTION ..... 1
- ACQUISITION ..... 2
  - Planning..... 2
  - Ground Survey..... 3
    - Monumentation ..... 3
    - RTK Surveys..... 4
    - Land Cover ..... 7
  - Airborne Survey..... 9
    - LiDAR..... 9
- PROCESSING ..... 10
  - LiDAR Data..... 10
- RESULTS & DISCUSSION ..... 12
  - LiDAR Density ..... 12
  - LiDAR Accuracy Assessments ..... 17
    - LiDAR Absolute Accuracy..... 17
    - LiDAR Vertical Relative Accuracy ..... 19
- SELECTED IMAGES..... 20
- GLOSSARY ..... 22
- APPENDIX A - ACCURACY CONTROLS ..... 23
- APPENDIX B – POINT DENSITIES..... 24
- APPENDIX C – ABSOLUTE AND RELATIVE ACCURACIES..... 34
- APPENDIX D – LANDCLASS ACCURACY STATISTICS ..... 44

**Cover Photo:** Bare-earth gridded model of channel network along Cottonwood Creek. The model is colored by elevation.



## INTRODUCTION

View from a location in the Swan NWR AOI in the Missoula Sites project in Montana.



In September 2013, WSI (Watershed Sciences, Inc.) was contracted by River Design Group, Inc. (RDG) to collect Light Detection and Ranging (LiDAR) data in the fall of 2013 for the Missoula Sites project in Montana. Data were collected to aid RDG in assessing the topographic and geophysical properties of the study area to support planning and development for river restoration and analysis.

This report accompanies the delivered LiDAR data and documents data acquisition procedures, processing methods, and results of all accuracy assessments for all Missoula Sites AOIs. Project specifics are shown in Table 1, the project extent can be seen in Figure 1, and a complete list of contracted deliverables provided to RDG can be found in Table 2.

**Table 1: Acquisition dates, acreages, and data types collected on the Missoula Sites site**

AOI	Contracted Acres	Buffered Acres	Acquisition Dates	Data Type
Brewer	560	836	10/04/2013	LiDAR
O'Dell	2,317	2,792	10/12/2013	LiDAR
Spook Lake	19	65	10/06/2013 10/10/2013	LiDAR
Piper	9,888	10,663	10/10/2013 10/11/2013	LiDAR
Shanley Creek	388	673	10/05/2013	LiDAR
Swan NWR	2,365	2,836	10/06/2013 10/10/2013	LiDAR
Nevada Creek	1,066	1,485	10/11/2013	LiDAR
Morrell Creek	347	576	10/06/2013 10/10/2013	LiDAR
Cottonwood Creek	824	1,183	10/06/2013 10/10/2013	LiDAR
Seeley Lake Nordic Ski Trail	928	1,525	10/06/2013 10/10/2013	LiDAR



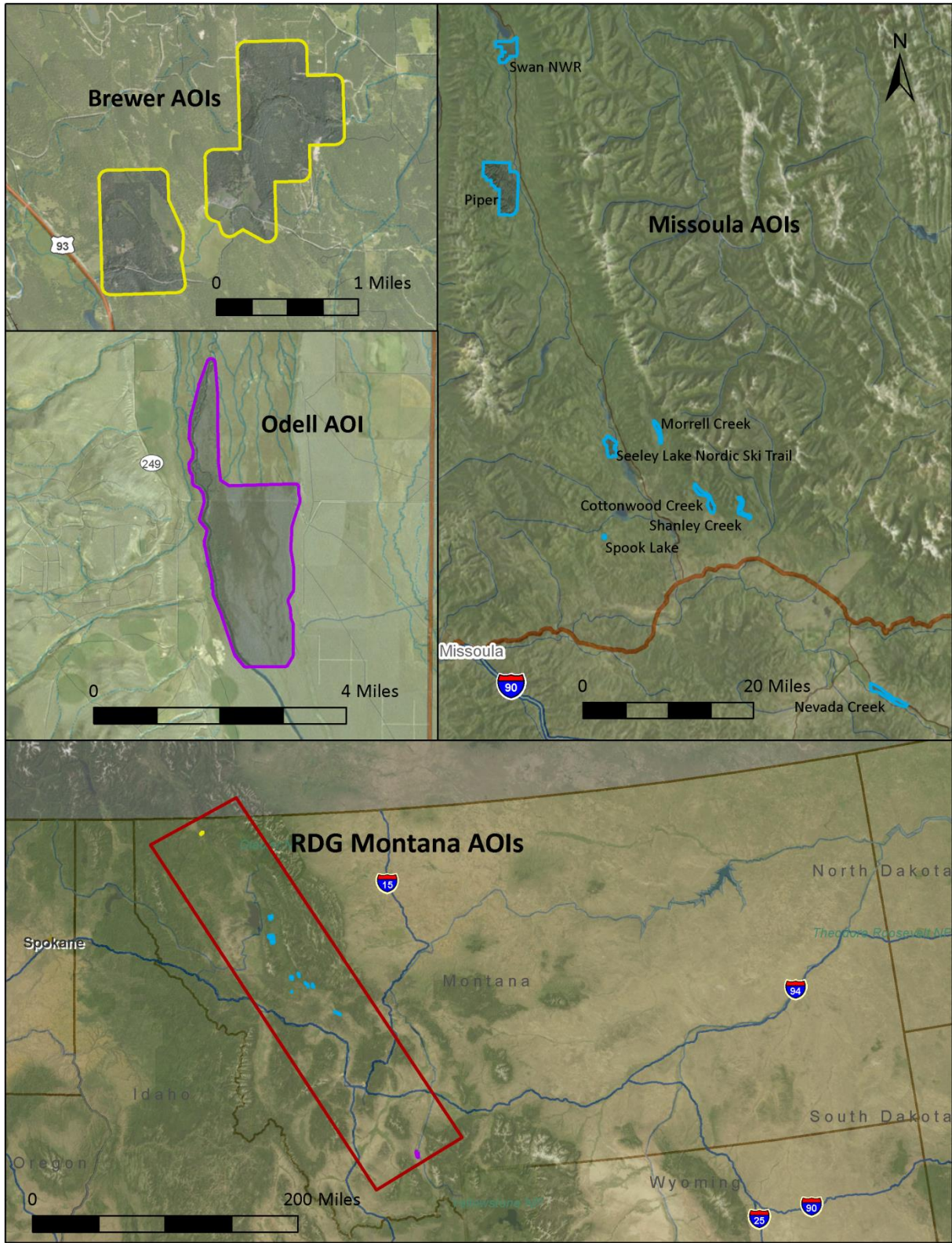


Figure 1: Location map of the Missoula Sites in Montana

**Table 2: Products delivered to RDG for the Missoula Sites project**

<b>Missoula Sites Products</b>	
<b>Projection: Montana State Plane Zone 2500</b>	
<b>Horizontal Datum: NAD83 (2011), Odell AOI: NAD83 (CORS96)</b>	
<b>Vertical Datum: NAVD88 (GEOID12A), Odell AOI: NAVD88 (GEOID03)</b>	
<b>Units: US Survey Feet</b>	
<b>LAS Files</b>	LAS v 1.2 <ul style="list-style-type: none"><li>• All Returns</li><li>• Model Keypoints</li></ul>
<b>Rasters</b>	3.0 Foot ESRI Grids <ul style="list-style-type: none"><li>• Bare Earth Model</li><li>• Highest Hit Model</li></ul> 1.5 Foot GeoTiffs <ul style="list-style-type: none"><li>• Intensity Images</li></ul>
<b>Vectors</b>	Shapefiles (*.shp) <ul style="list-style-type: none"><li>• Site Boundary</li><li>• LiDAR Index</li><li>• DEM/DSM Index</li></ul>

WSI field vehicle supporting acquisition in the Morrell Creek site.



## Planning

In preparation for data collection, WSI reviewed the project area using Google Earth, and flightlines were developed using a combination of specialized software. Careful planning by acquisition staff entailed adapting the pulse rate, flight altitude, scan angle, and ground speed to ensure complete coverage of the Missoula Sites LiDAR study area at the target point density of  $\geq 8$  pulses per square meter (0.74 pulses/square foot). Efforts are taken to optimize flight paths by minimizing flight times while meeting all accuracy specifications.

Factors such as satellite constellation availability and weather windows must be considered during the planning stage. Any weather hazards or conditions affecting the flights were continuously monitored due to their potential impact on the daily success of airborne and ground operations.

## Ground Survey

Ground survey data are used to geospatially correct the aircraft positional coordinate data and to perform quality assurance checks on final LiDAR data. Ground surveys, including monumentation and ground check points, are conducted to support the airborne acquisition process.



## Monumentation

The spatial configuration of ground survey monuments provided redundant control within 13 nautical miles of the mission areas for LiDAR flights. Monuments were also used for collection of ground control points using RTK survey techniques (see **RTK** below).

Monument locations were selected with consideration for satellite visibility, field crew safety, and optimal location for RTK coverage. WSI established one new monument and utilized eight existing monuments for the Missoula Sites project (Table 3, Figure 2). New monumentation was set using 5/8" x 30" rebar topped with stamped 2" aluminum caps. RDG's professional land surveyor, Andrew Belski (MTPLS# PEL-LS-LIC-14731) oversaw and certified the establishment of all monuments.

**Table 3: Monuments utilized for the Missoula Sites acquisition. Coordinates are on the NAD83 (2011) datum, epoch 2010.00**

Monument ID	Latitude	Longitude	Ellipsoid (meters)
BREWER_1	48° 50' 08.46337"	-114° 56' 14.67052"	844.909
BREWER_2	48° 50' 08.49728"	-114° 56' 14.39981"	844.928
COTTONWOOD_1	47° 08' 57.62032"	-113° 18' 53.95694"	1393.641
ENNIS_1 (a.k.a ODELL_1)	45° 16' 07.82737"	-111° 39' 05.22474"	1616.928
ENNIS_2	45° 16' 07.56615"	-111° 39' 05.34346"	1616.876
MORRELL_1	47° 15' 53.43601"	-113° 26' 53.95863"	1396.625
NEVADA_CRK_1	46° 48' 12.03149"	-112° 48' 35.99078"	1398.621
NEVADA_CRK_2	46° 48' 11.62939"	-112° 48' 35.98490"	1398.936
PIPER_1	47° 39' 34.52005"	-113° 50' 31.19071"	1121.312
SHANLEY_1	47° 08' 44.10677"	-113° 14' 15.00377"	1553.982
SHANLEY_2	47° 08' 45.08570"	-113° 14' 17.27387"	1556.169
SPOOK_1	47° 04' 30.79832"	-113° 33' 00.90302"	1670.317
SWAN_1	47° 54' 24.40776"	-113° 50' 20.15799"	921.637
WSBP_1	47° 13' 16.51887"	-113° 32' 54.75224"	1220.173

To correct the continuous onboard measurements of the aircraft position recorded throughout the missions, WSI concurrently conducted multiple static Global Navigation Satellite System (GNSS) ground surveys (1 Hz recording frequency) over each monument. After the airborne survey, the static GPS data were triangulated with nearby Continuously Operating Reference Stations (CORS) using the Online Positioning User Service (OPUS<sup>1</sup>) for precise positioning. Multiple independent sessions over the same monument were processed to confirm antenna height measurements and to refine position accuracy.

## RTK Surveys

For the real time kinematic (RTK) check point data collection, a Trimble R7 base unit was positioned at a nearby monument to broadcast a kinematic correction to a roving Trimble R10 receiver. All RTK measurements were made during periods with a Position Dilution of Precision (PDOP) of  $\leq 3.0$  with at least six satellites in view of the stationary and roving receivers. When collecting RTK data, the rover would record data while stationary for five seconds, then calculate the pseudorange position using at least three one-second epochs. Relative errors for the position must be less than 1.5 cm horizontal and 2.0 cm vertical in order to be accepted. See Table 4 for Trimble unit specifications.

RTK positions were collected on paved roads and other hard surface locations such as gravel or stable dirt roads that also had good satellite visibility. RTK measurements were not taken on highly reflective surfaces such as center line stripes or lane markings on roads due to the increased noise seen in the laser returns over these surfaces. The distribution of RTK points depended on ground access constraints and may not be equitably distributed throughout the study area. See Figure 2 and Figure 3 for the distribution of RTK in this project.

**Table 4: Trimble equipment identification**

Receiver Model	Antenna	OPUS Antenna ID	Use
Trimble R7 GNSS	Zephyr GNSS Geodetic Model 2 RoHS	TRM57971.00	Static
Trimble R10	Integrated Antenna R10	TRMR10	Static, RTK

---

<sup>1</sup> OPUS is a free service provided by the National Geodetic Survey to process corrected monument positions. <http://www.ngs.noaa.gov/OPUS>.

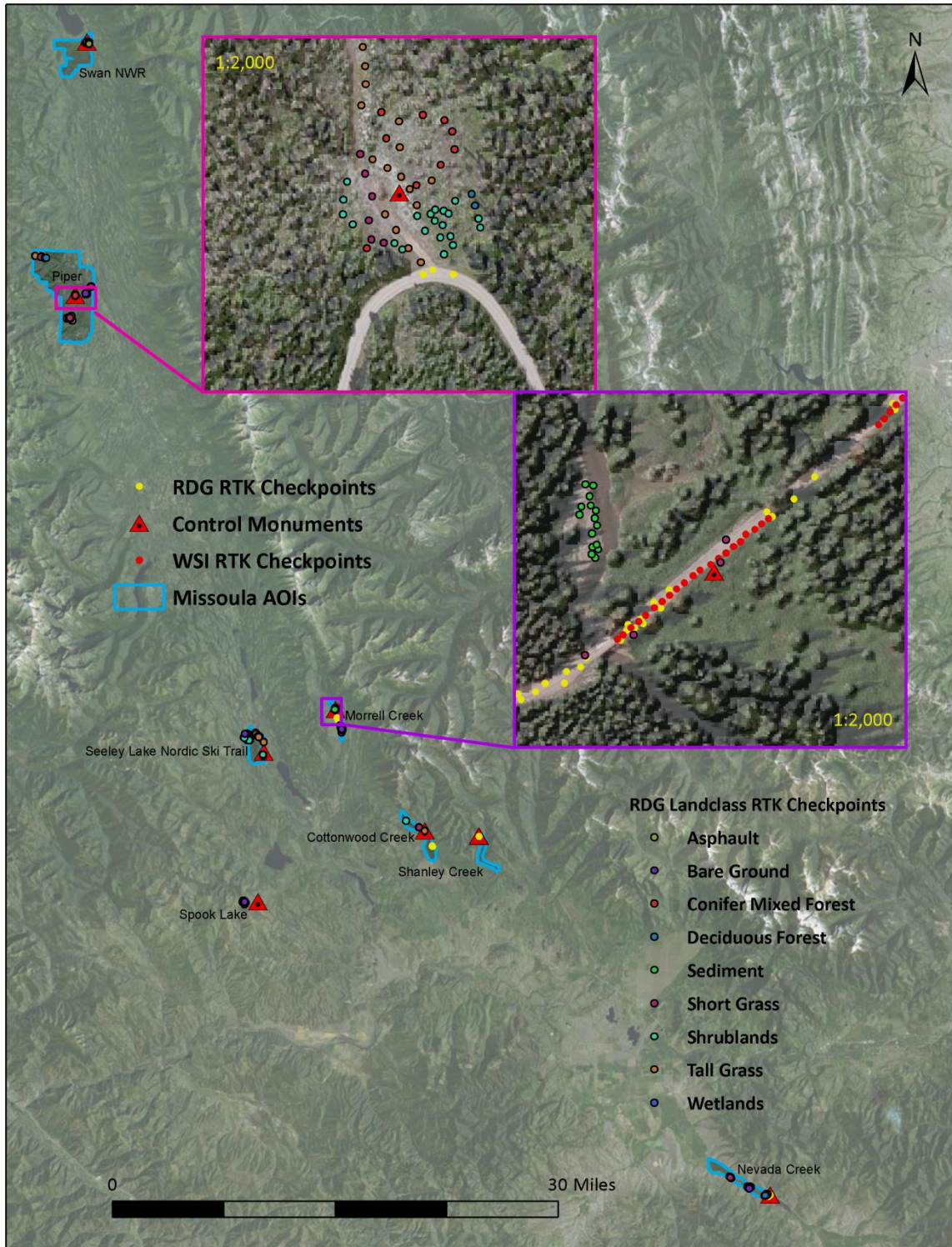


Figure 2: Missoula AOIs basestation, landclass, and RTK checkpoint location map

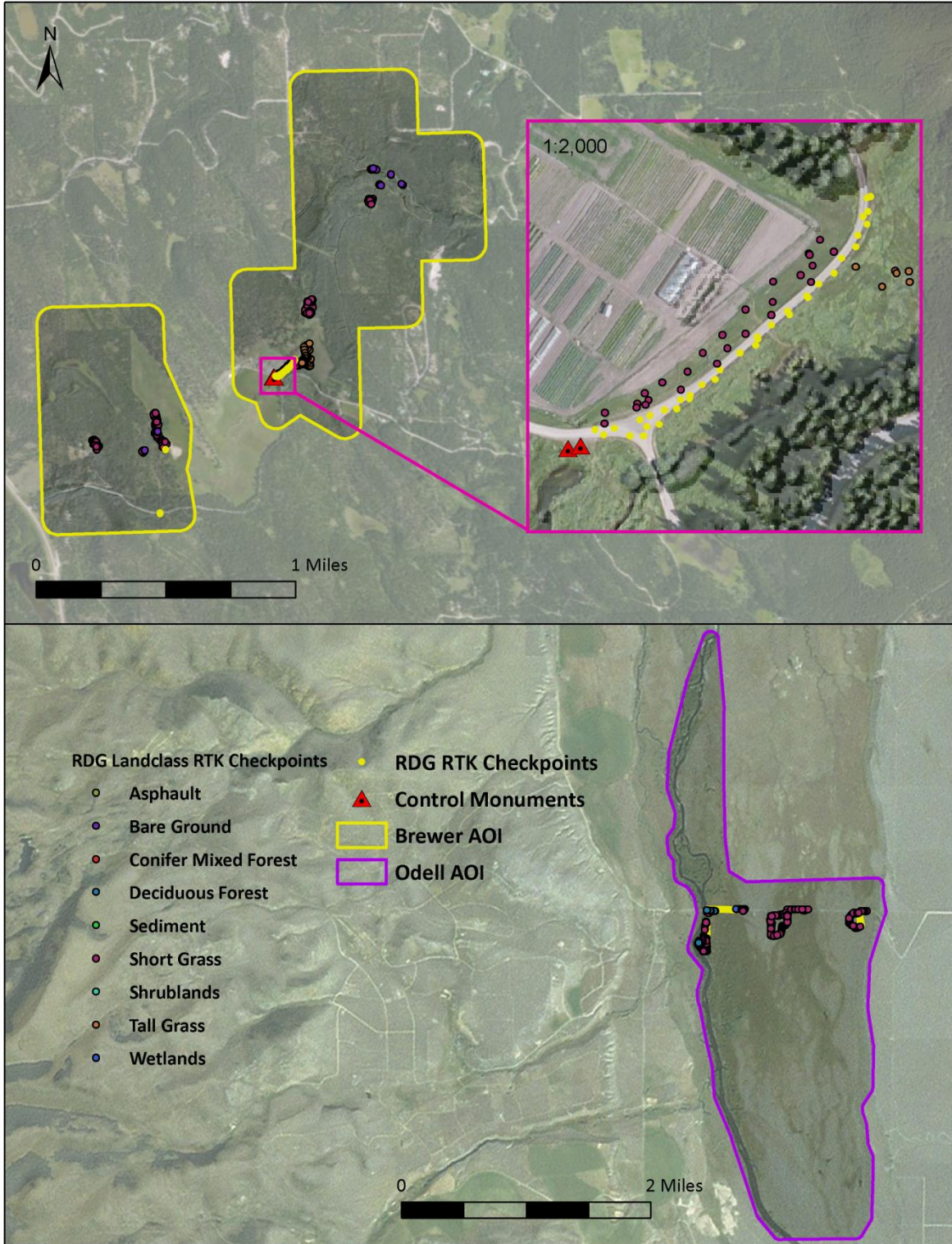


Figure 3: Brewer and Odell AOIs basestation, landclass RTK and RTK checkpoint location map

## Land Cover

In addition to control point RTK, landclass check points were taken throughout the study area. Landclass cover types, codes and USGS established descriptions can be found in Table 5.<sup>2</sup> Individual accuracies were calculated for each land-cover class type to assess confidence in the LiDAR derived ground models across land cover classes, and can be found in Table 11.

**Table 5: Land cover class descriptions of check points taken for the Missoula Sites AOIs**

Land cover type	Applicable RDG land cover codes	USGS Description
Bare Earth	TOPO FL, TOPO, grnd w/ bark, gravel/dirt, gravel, dirt-gravel, dirt, bare ground, bare grnd, bare dirt	Areas characterized by bare rock, gravel, sand, silt, clay, or other earthen material, with little or no “green” vegetation present regardless of its inherent ability to support life.
Short Grass	grass, 1.5 ft grass, cl 2in grass, gravel/grass, 0.5ft mowed grass, 1ft bear grass, 0.5ft grass, 1in grass, cl 2in grass, 1.5 ft weeds/gravel, grass/gravel, GRASS, WHEAT 1' HIGH	Vegetation planted in developed settings for recreation, erosion control, or aesthetic purposes.
Tall Grass	2ft grass, 3ft grass, GRASS 2'/KNAPWEED, GRASS 3', GRASS 3'/KNAPWEED, UPLAND GRASS 3'/KNAPWEED, up grass, upland grass, topo 2.5ft grass, topo 3ft grass, topo 4ft grass, gravel / knapweed, knapwee., upland grass/knapweed, 4ft grass, gravel/2.5ft grass, gravel/2ft grass, gravel/wheat.	Areas dominated by upland grasses and forbs. Herbaceous vegetation accounts for 75-100 percent of the cover
Wetlands	WETLAND VEG, SEDGE, SEDGE/WILLOW, wetland veg, sedge, SEDGE/MULLEN, topo 3ft sedges, wetland veg/moss, topo cat tails, wetland grass 2.5ft	Areas where the soil or substrate is periodically saturated with or covered with water as defined by Cowardin et al.
Deciduous Forest	WILLOWS, willows, dogwood, willow, cottonwod/shrub mix	Areas dominated by trees where 75 percent or more of the tree species shed foliage simultaneously in response to seasonal change.
Conifer/Mixed Forest	6ft lodgepole, aspen/larch, fir tree, knapweed/larch, larch, pine tree	Areas dominated by trees where neither deciduous nor evergreen species represent more than 75 percent of the cover present.

<sup>2</sup> The USGS Land Cover Institute, NLCD 92 Land Cover Class Definitions. December 2012. Accessed 21 November 2013. <<http://landcover.usgs.gov/classes.php>>.

Land cover type	Applicable RDG land cover codes	USGS Description
Shrubland	Thistle, sage, shrub, 3ft shrubs, bare ground 1.5ft mullan, rosehip bush, huck plant, huckleberry plant, shrub, 7ft bush, mullen, thistle, thistle/mullen, broadleaf plant 3ft, fern, shrub/grass, GRASS PASTURE	Areas dominated by shrubs; shrub canopy accounts for 25-100 percent of the cover.
Sediment	4in- alluvium, mud	Perennially barren areas of bedrock, desert pavement, scarps, talus, slides, volcanic material, debris, beaches, or earthen material.
Asphalt	cl path conc, cor conc, edg conc, eo,	Areas with extractive mining activities or surface depression.

# Airborne Survey

## LiDAR

The LiDAR survey was accomplished with a Leica ALS60 system mounted in a Partenavia airplane. Table 6 summarizes the settings used to yield an average pulse density of  $\geq 8$  pulses/m<sup>2</sup> over the Missoula Sites terrain. It is not uncommon for some types of surfaces (e.g. dense vegetation or water) to return fewer pulses to the LiDAR sensor than the laser originally emitted. These discrepancies between native and delivered density will vary depending on terrain, land cover, and the prevalence of water bodies.

**Table 6: LiDAR specifications and survey settings**

LiDAR Survey Settings & Specifications	
Sensor	Leica ALS60
Survey Altitude (AGL)	900 m
Target Pulse Rate	95-106 kHz
Sensor Configuration	Single Pulse in Air (SPiA)
Laser Pulse Diameter	21 cm
Field of View	26°
GPS Baselines	$\leq 13$ nm
GPS PDOP	$\leq 3.0$
GPS Satellite Constellation	$\geq 6$
Maximum Returns	4
Intensity	8-bit
Resolution/Density	Average 8 pulses/m <sup>2</sup>
Accuracy	RMSE <sub>z</sub> $\leq 15$ cm

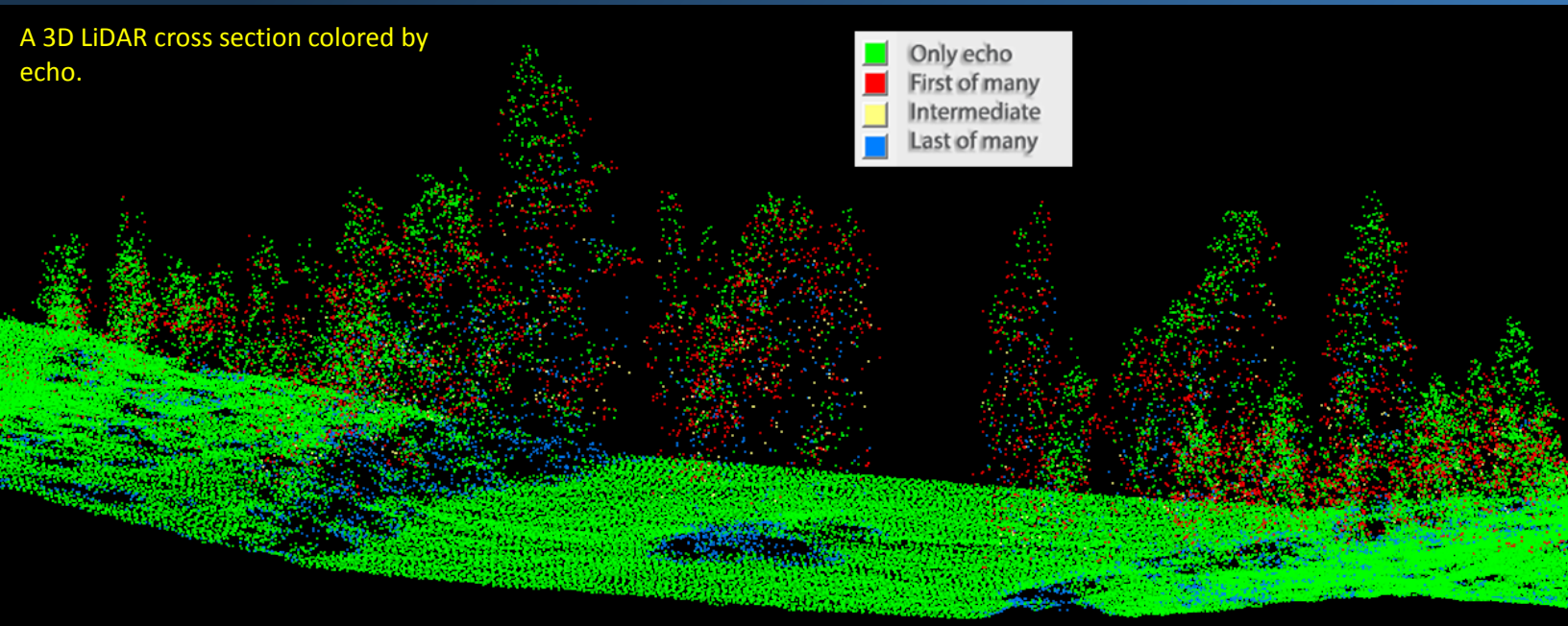
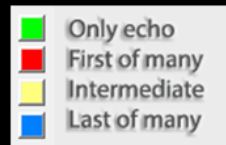
**Leica ALS60 LiDAR sensor**



To reduce laser shadowing and increase surface laser painting, all areas were surveyed with an opposing flight line side-lap of  $\geq 50\%$  ( $\geq 100\%$  overlap). The Leica laser systems record up to four range measurements (returns) per pulse. All discernible laser returns were processed for the output dataset.

To accurately solve for laser point position (geographic coordinates  $x, y, z$ ), the positional coordinates of the airborne sensor and the attitude of the aircraft were recorded continuously throughout the LiDAR data collection mission. Position of the aircraft was measured twice per second (2 Hz) by an onboard differential GPS unit. Aircraft attitude was measured 200 times per second (200 Hz) as pitch, roll, and yaw (heading) from an onboard inertial measurement unit (IMU). To allow for post-processing correction and calibration, aircraft/sensor position and attitude data are indexed by GPS time.

A 3D LiDAR cross section colored by echo.



## LiDAR Data

Upon the LiDAR data’s arrival to the office, WSI processing staff initiates a suite of automated and manual techniques to process the data into the requested deliverables. Processing tasks include GPS control computations, smoothed best estimate trajectory (SBET) calculations, kinematic corrections, calculation of laser point position, calibration for optimal relative and absolute accuracy, and classification of ground and non-ground points (Table 7). Processing methodologies are tailored for the landscape and intended application of the point data. A full description of these tasks can be found in Table 8.

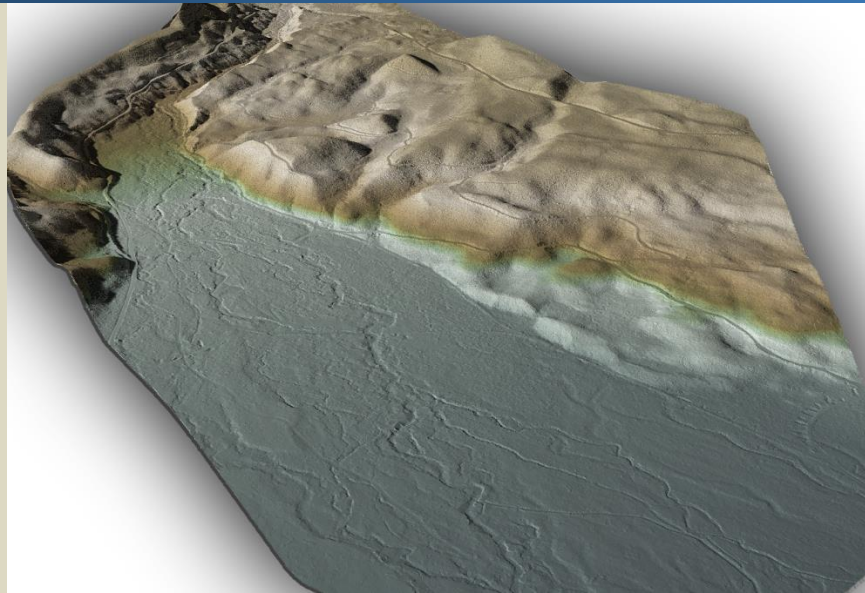
**Table 7: ASPRS LAS classification standards applied to the Missoula Sites dataset**

Classification Number	Classification Name	Classification Description
1	Default/ Unclassified	Laser returns that are not included in the ground class and not dismissed as Noise or Withheld points
2	Ground	Ground that is determined by a number of automated and manual cleaning algorithms to determine the best ground model the data can support
8	Model Key Points	Previously classified ground points, thinned using a spacing of 20 feet and vertical tolerances of 0.1 ft., 0.2 ft., 0.5 ft., and 1 ft.

**Table 8: LiDAR processing workflow**

LiDAR Processing Step	Software Used
Resolve kinematic corrections for aircraft position data using kinematic aircraft GPS and static ground GPS data.	Waypoint GPS v.8.3 Trimble Business Center v.3.00 Geographic Calculator 2013
Develop a smoothed best estimate of trajectory (SBET) file that blends post-processed aircraft position with attitude data. Sensor head position and attitude are calculated throughout the survey. The SBET data are used extensively for laser point processing.	IPAS TC v.3.1
Calculate laser point position by associating SBET position to each laser point return time, scan angle, intensity, etc. Create raw laser point cloud data for the entire survey in *.las (ASPRS v. 1.2) format. Data are converted to orthometric elevations (NAVD88) by applying a Geoid12 correction.	ALS Post Processing Software v.2.74
Import raw laser points into manageable blocks (less than 500 MB) to perform manual relative accuracy calibration and filter erroneous points. Ground points are then classified for individual flight lines (to be used for relative accuracy testing and calibration).	TerraScan v.13.008
Using ground classified points per each flight line, the relative accuracy is tested. Automated line-to-line calibrations are then performed for system attitude parameters (pitch, roll, heading), mirror flex (scale) and GPS/IMU drift. Calibrations are calculated on ground classified points from paired flight lines and results are applied to all points in a flight line. Every flight line is used for relative accuracy calibration.	TerraMatch v.13.002
Classify resulting data to ground and other client designated ASPRS classifications (Table 7). Assess statistical absolute accuracy via direct comparisons of ground classified points to ground RTK survey data.	TerraScan v.13.008 TerraModeler v.13.002
Generate bare earth models as triangulated surfaces. Highest hit models were created as a surface expression of all classified points (excluding the noise and withheld classes). All surface models were exported as ESRI Grids at a 3 foot pixel resolution.	TerraScan v.13.008 ArcMap v. 10.1 TerraModeler v.13.002

Bare-earth gridded model of Fawn Creek looking northwest. The model is colored by elevation.



### LiDAR Density

The sensor is set to acquire a native density of 8 points/m<sup>2</sup>. Depending on the nature of the terrain, the first returned echo will be the highest hit surface. In vegetated areas, the first return surface will represent the top of the canopy, while in clearings or on paved roads, the first return surface will represent the ground. The ground density differs from the first return density due to the fact that in vegetated areas, fewer returns may penetrate the canopy. The ground classification is generally determined by first echo returns in non-vegetated areas combined with last echo returns in vegetated areas. The pulse density distribution will vary within the study area due to laser scan pattern and flight conditions. Additionally, some types of surfaces (i.e. breaks in terrain, water, steep slopes) may return fewer pulses to the sensor than originally emitted by the laser.

The cumulative average first-return density for the LiDAR data for the Missoula Sites was 0.96 points/ft<sup>2</sup> (10.38 points/m<sup>2</sup>) while the cumulative average ground classified density was 0.21 points/ft<sup>2</sup> (2.20 points/m<sup>2</sup>) (Table 9). The statistical distribution of first returns (Figure 4) and classified ground points (Figure 5) are portrayed below. Also presented are the spatial distribution of average first return densities (Figure 6) and ground point densities (Figure 7) for each 100mx100m cell. Additional frequency distributions of ground and first returns point densities by AOI can be found in Appendix B.

**Table 9: Average LiDAR point densities**

AOI	First Return Point Densities	Ground Point Densities
<b>Cumulative</b>	<b>0.96 points/ft<sup>2</sup></b> <b>10.38 points/m<sup>2</sup></b>	<b>0.21 points/ft<sup>2</sup></b> <b>2.20 points/m<sup>2</sup></b>
<b>Brewer</b>	0.99 points/ft <sup>2</sup> 10.65 points/m <sup>2</sup>	0.23 points/ft <sup>2</sup> 2.48 points/m <sup>2</sup>
<b>O'Dell Creek</b>	0.84 points/ft <sup>2</sup> 9.07 points/m <sup>2</sup>	0.54 points/ft <sup>2</sup> 5.82 points/m <sup>2</sup>
<b>Cottonwood Creek</b>	0.86 points/ft <sup>2</sup> 9.30 points/m <sup>2</sup>	0.14 points/ft <sup>2</sup> 1.51 points/m <sup>2</sup>
<b>Morrell Creek</b>	1.48 points/ft <sup>2</sup> 15.88 points/m <sup>2</sup>	0.20 points/ft <sup>2</sup> 2.16 points/m <sup>2</sup>
<b>Nevada Creek</b>	0.99 points/ft <sup>2</sup> 10.72 points/m <sup>2</sup>	0.34 points/ft <sup>2</sup> 3.62 points/m <sup>2</sup>
<b>Piper</b>	0.96 points/ft <sup>2</sup> 1.35 points/m <sup>2</sup>	0.12 points/ft <sup>2</sup> 1.31 points/m <sup>2</sup>
<b>Shanley Creek</b>	1.04 points/ft <sup>2</sup> 11.18 points/m <sup>2</sup>	0.18 points/ft <sup>2</sup> 1.90 points/m <sup>2</sup>
<b>Spook Creek</b>	1.20 points/ft <sup>2</sup> 12.90 points/m <sup>2</sup>	0.15 points/ft <sup>2</sup> 1.62 points/m <sup>2</sup>
<b>Swan NWR</b>	0.94 points/ft <sup>2</sup> 10.11 points/m <sup>2</sup>	0.15 points/ft <sup>2</sup> 1.57 points/m <sup>2</sup>
<b>Seeley Lake Nordic Ski Trail</b>	1.05 points/ft <sup>2</sup> 11.27 points/m <sup>2</sup>	0.20 points/ft <sup>2</sup> 2.19 points/m <sup>2</sup>

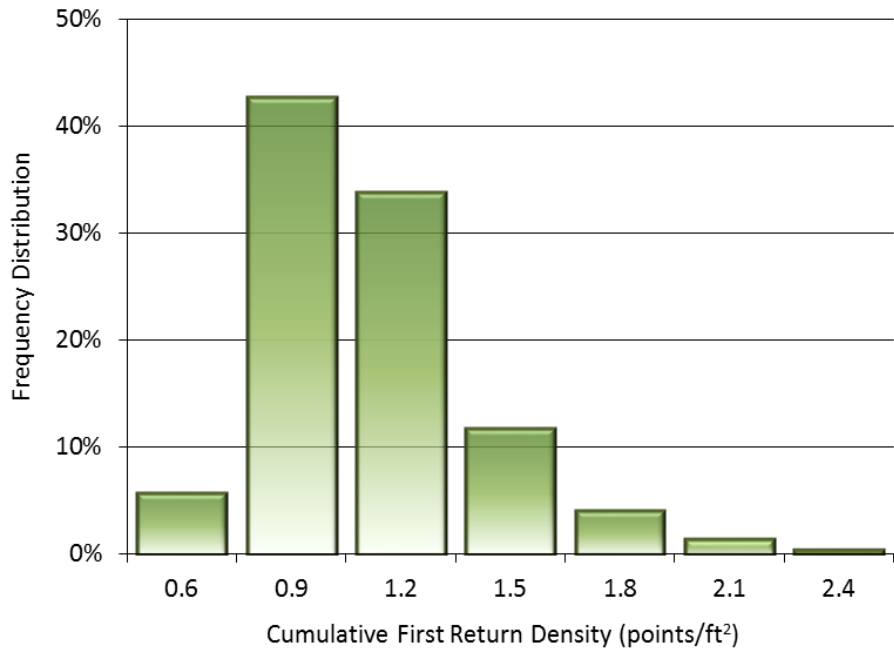


**Figure 4: Cumulative frequency distribution of first return densities (native densities) of the gridded study area**

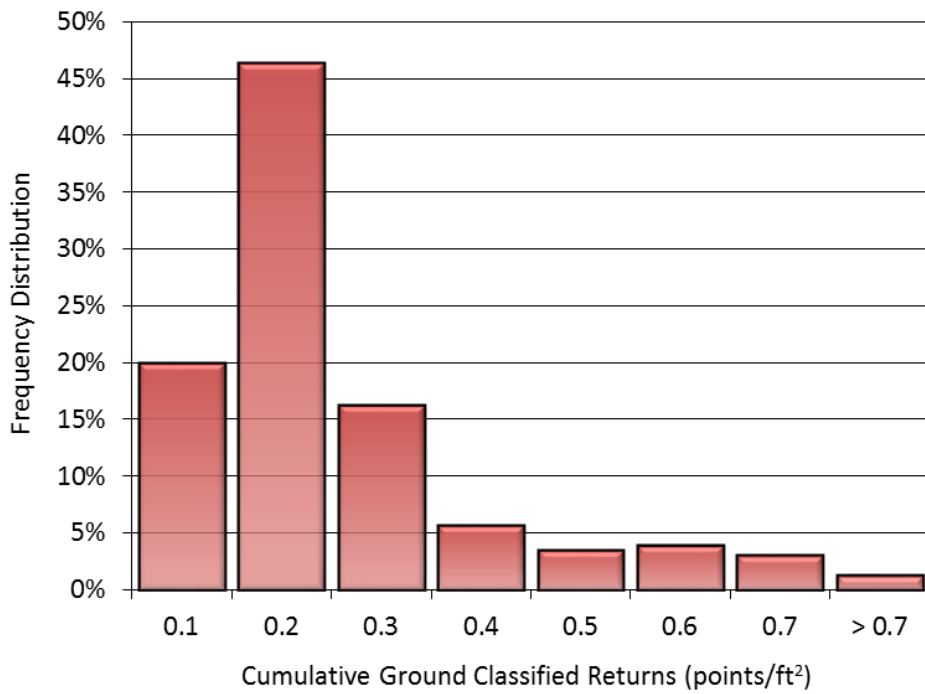


**Figure 5: Cumulative frequency distribution of ground return densities of the gridded study area**

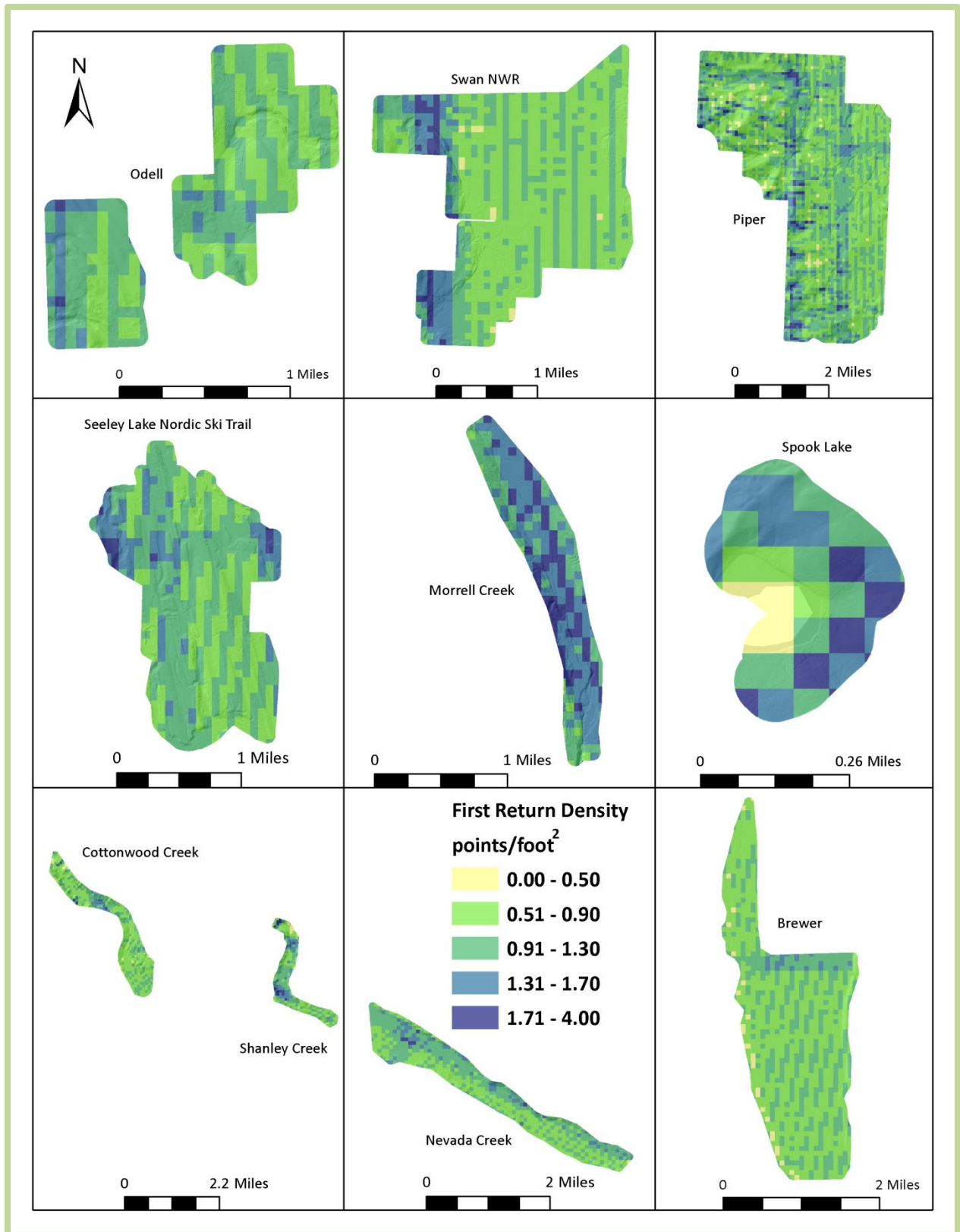
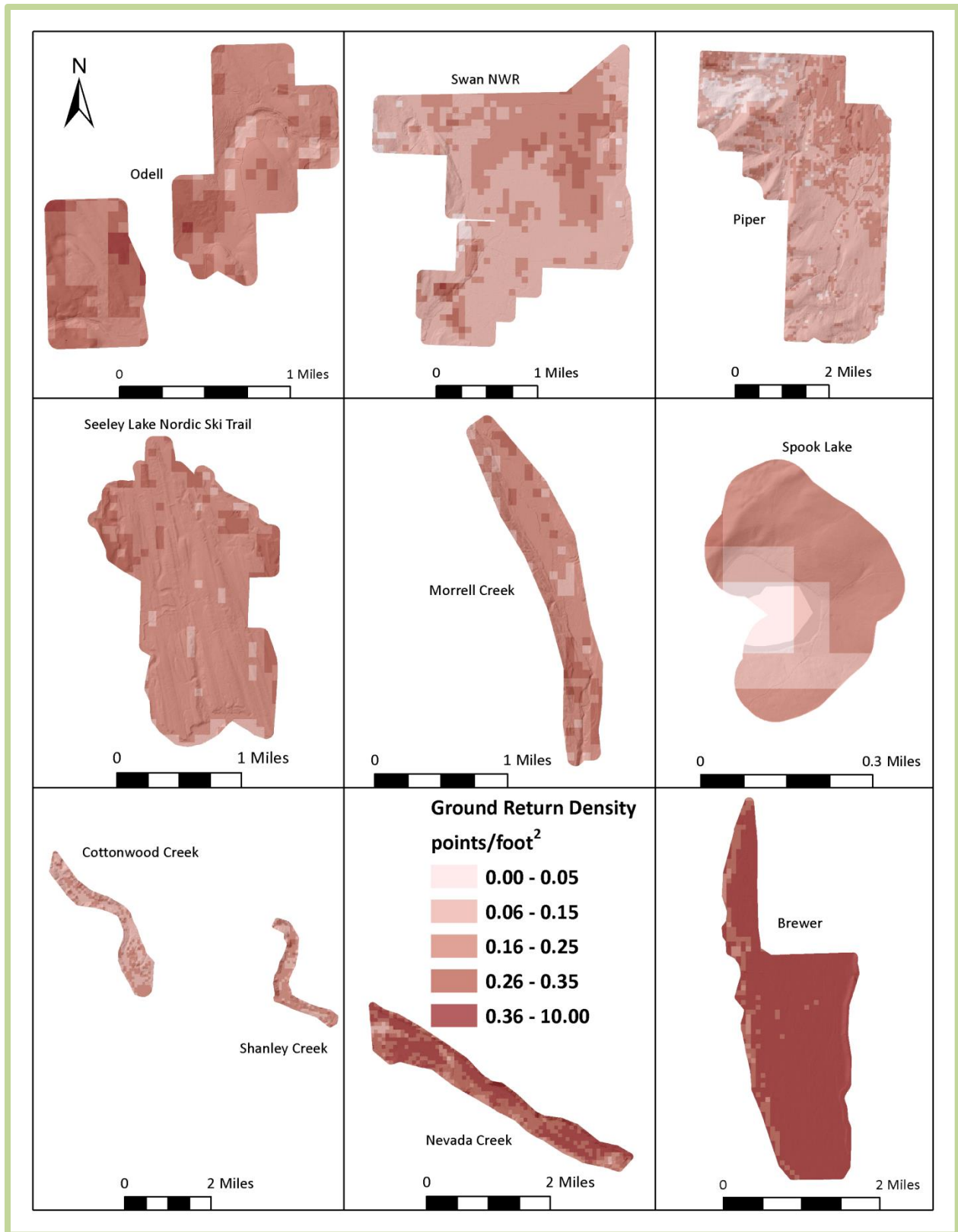


Figure 6: Native density map for the Missoula Sites site (100mx100m cells)



**Figure 7: Ground density map for the Missoula Sites site (100mx100m cells)**

## LiDAR Accuracy Assessments

The accuracy of the LiDAR data collection can be described in terms of absolute accuracy (the consistency of the data with external data sources) and relative accuracy (the consistency of the dataset with itself). See Appendix A for further information on sources of error and operational measures used to improve relative accuracy.

### LiDAR Absolute Accuracy

Vertical absolute accuracy was primarily assessed from RTK ground check point (GCP) data collected on open, bare earth surfaces with level slope (<20°). Fundamental Vertical Accuracy (FVA) reporting is designed to meet guidelines presented in the FGDC National Standard for Spatial Data Accuracy<sup>3</sup>. FVA compares known RTK ground survey check points to the triangulated ground surface generated by the LiDAR points. FVA is a measure of the accuracy of LiDAR point data in open areas where the LiDAR system has a “very high probability” of measuring the ground surface and is evaluated at the 95% confidence interval (1.96  $\sigma$ ).

Absolute accuracy is described as the mean and standard deviation (sigma  $\sigma$ ) of divergence of the ground surface model from ground survey point coordinates. These statistics assume the error for x, y, and z is normally distributed, and therefore the skew and kurtosis of distributions are also considered when evaluating error statistics. For the Missoula Sites survey, 558 RTK points were collected in total resulting in a cumulative average accuracy of 0.006 feet (0.002 meters) (Table 10, Figure 8). Absolute accuracies calculated by Land Class RTK checkpoints can be found in Table 11. Absolute and relative accuracy frequency histograms can be found in Appendix C, while Land Class absolute accuracy frequency histograms can be found in Appendix D.

**Table 10: Cumulative absolute and relative accuracies**

	Sample	Average	Median	RMSE	Standard Deviation (1 $\sigma$ )	1.96 $\sigma$
<b>Absolute Accuracy</b>	558 points	-0.006 ft	-0.003 ft	0.071 ft	0.071 ft	0.139 ft
		-0.002 m	-0.001 m	0.022 m	0.022 m	0.042 m
<b>Relative Accuracy</b>	217 surfaces	0.122 ft	0.141 ft	0.144 ft	0.035 ft	0.070 ft
		0.037 m	0.043 m	0.044 m	0.011 m	0.021 m

<sup>3</sup> Federal Geographic Data Committee, Geospatial Positioning Accuracy Standards (FGDC-STD-007.3-1998). Part 3: National Standard for Spatial Data Accuracy. <http://www.fgdc.gov/standards/projects/FGDC-standards-projects/accuracy/part3/chapter3>

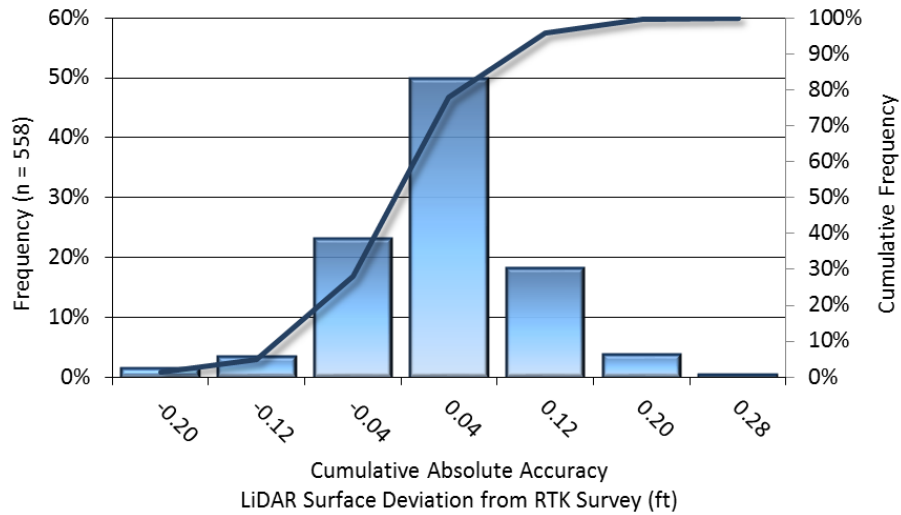


**Figure 8: Frequency histogram for LiDAR surface deviation from RTK values**

**Table 11: Land Class RTK absolute accuracies**

Absolute Accuracies by Landclass RTK						
Landclass	Sample	Average	Median	RMSE	Standard Deviation (1σ)	1.96σ
Bare Earth	74 points	0.004 ft	0.025 ft	0.275 ft	0.277 ft	0.543 ft
		0.001 m	0.008 m	0.084 m	0.084 m	0.166 m
Short Grass	748 points	0.086 ft	0.072 ft	0.200 ft	0.181 ft	0.354 ft
		0.026 m	0.022 m	0.061 m	0.055 m	0.108 m
Tall Grass	697 points	0.054 ft	0.040 ft	0.107 ft	0.093 ft	0.182 ft
		0.016 m	0.012 m	0.033 m	0.028 m	0.055 m
Wetlands	141 points	0.382 ft	0.374 ft	0.437 ft	0.214 ft	0.420 ft
		0.116 m	0.114 m	0.133 m	0.065 m	0.128 m
Deciduous Forest	29 points	0.153 ft	0.157 ft	0.219 ft	0.158 ft	0.311 ft
		0.047 m	0.048 m	0.067 m	0.048 m	0.095 m
Mixed Forest	28 points	0.084 ft	0.108 ft	0.202 ft	0.187 ft	0.367 ft
		0.026 m	0.033 m	0.062 m	0.057 m	0.112 m
Shrubland	120 points	0.179 ft	0.138 ft	0.301 ft	0.243 ft	0.475 ft
		0.055 m	0.042 m	0.092 m	0.074 m	0.145 m
Sediment	35 points	-0.021 ft	-0.020 ft	0.119 ft	0.119 ft	0.233 ft
		-0.007 m	-0.006 m	0.036 m	0.036 m	0.071 m
Asphalt	33 points	-0.060 ft	-0.056 ft	0.126 ft	0.113 ft	0.221 ft
		-0.018 m	-0.017 m	0.038 m	0.034 m	0.067 m

## LiDAR Vertical Relative Accuracy

Relative vertical accuracy refers to the internal consistency of the data set as a whole: the ability to place an object in the same location given multiple flight lines, GPS conditions, and aircraft attitudes. When the LiDAR system is well calibrated, the swath-to-swath vertical divergence is low (<0.10 meters). The relative vertical accuracy is computed by comparing the ground surface model of each individual flight line with its neighbors in overlapping regions. The average (mean) line to line relative vertical accuracy for the Missoula Sites was 0.122 feet (0.037 meters). (Table 10, Figure 9).

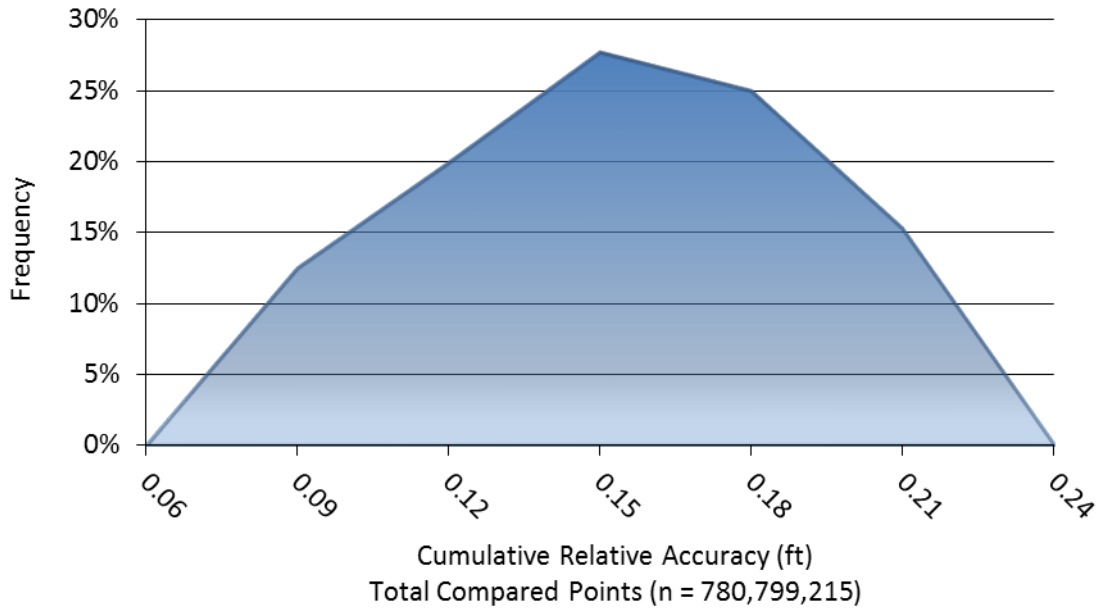


**Figure 9: Frequency plot for relative vertical accuracy between flight lines**



**Figure 10:** A Stacked view of the Cottonwood Creek AOI. The left image is the bare-earth model colored by elevation, the right image is the 3D LiDAR point cloud draped with NAIP imagery.



Figure 11: 3D LiDAR point cloud of Seeley Lake. The model is draped with NAIP imagery.

**1-sigma ( $\sigma$ ) Absolute Deviation:** Value for which the data are within one standard deviation (approximately 68<sup>th</sup> percentile) of a normally distributed data set.

**1.96-sigma ( $\sigma$ ) Absolute Deviation:** Value for which the data are within two standard deviations (approximately 95<sup>th</sup> percentile) of a normally distributed data set.

**Accuracy:** The statistical comparison between known (surveyed) points and laser points. Typically measured as the standard deviation ( $\sigma$ ) and root mean square error (RMSE).

**Absolute Accuracy:** The vertical accuracy of LiDAR data is described as the mean and standard deviation ( $\sigma$ ) of divergence of LiDAR point coordinates from RTK ground survey point coordinates. To provide a sense of the model predictive power of the dataset, the root mean square error (RMSE) for vertical accuracy is also provided. These statistics assume the error distributions for x, y, and z are normally distributed, thus we also consider the skew and kurtosis of distributions when evaluating error statistics.

**Relative Accuracy:** Relative accuracy refers to the internal consistency of the data set - the ability to place a laser point in the same location over multiple flight lines, GPS conditions, and aircraft attitudes. Affected by system attitude offsets, scale, and GPS/IMU drift, internal consistency is measured as the divergence between points from different flight lines within an overlapping area. Divergence is most apparent when flight lines are opposing. When the LiDAR system is well calibrated, the line-to-line divergence is low (<10 cm).

**Root Mean Square Error (RMSE):** A statistic used to approximate the difference between real-world points and the LiDAR points. It is calculated by squaring all the values, then taking the average of the squares and taking the square root of the average.

**Data Density:** A common measure of LiDAR resolution, measured as points per square meter.

**DTM / DEM:** These often-interchanged terms refer to models made from laser points. The digital elevation model (DEM) refers to all surfaces, including bare ground and vegetation, while the digital terrain model (DTM) refers only to those points classified as ground.

**Intensity Values:** The peak power ratio of the laser return to the emitted laser. It is a function of surface reflectivity.

**Laser Noise:** For any given target, laser noise is the breadth of the data cloud per laser return (i.e., last, first, etc.). Lower intensity surfaces (roads, rooftops, still/calm water) experience higher laser noise.

**Nadir:** A single point or locus of points on the surface of the earth directly below a sensor as it progresses along its flight line.

**Overlap:** The area shared between flight lines, typically measured in percent; 100% overlap is essential to ensure complete coverage and reduce laser shadows.

**Pulse Rate (PR):** The rate at which laser pulses are emitted from the sensor; typically measured as thousands of pulses per second (kHz).

**Pulse Returns:** For every laser pulse emitted, the Leica ALS 60 system can record *up to four* wave forms reflected back to the sensor. Portions of the wave form that return earliest are the highest element in multi-tiered surfaces such as vegetation. Portions of the wave form that return last are the lowest element in multi-tiered surfaces.

**Real-Time Kinematic (RTK) Survey:** GPS surveying is conducted with a GPS base station deployed over a known monument with a radio connection to a GPS rover. Both the base station and rover receive differential GPS data and the baseline correction is solved between the two. This type of ground survey is accurate to 1.5 cm or less.

**Scan Angle:** The angle from nadir to the edge of the scan, measured in degrees. Laser point accuracy typically decreases as scan angles increase.

**Spot Spacing:** Also a measure of LiDAR resolution, measured as the average distance between laser points.

## APPENDIX A - ACCURACY CONTROLS

### Relative Accuracy Calibration Methodology:

**Manual System Calibration:** Calibration procedures for each mission require solving geometric relationships that relate measured swath-to-swath deviations to misalignments of system attitude parameters. Corrected scale, pitch, roll and heading offsets were calculated and applied to resolve misalignments. The raw divergence between lines was computed after the manual calibration was completed and reported for each survey area.

**Automated Attitude Calibration:** All data were tested and calibrated using TerraMatch automated sampling routines. Ground points were classified for each individual flight line and used for line-to-line testing. System misalignment offsets (pitch, roll and heading) and scale were solved for each individual mission and applied to respective mission datasets. The data from each mission were then blended when imported together to form the entire area of interest.

**Automated Z Calibration:** Ground points per line were used to calculate the vertical divergence between lines caused by vertical GPS drift. Automated Z calibration was the final step employed for relative accuracy calibration.

### LiDAR accuracy error sources and solutions:

Type of Error	Source	Post Processing Solution
GPS (Static/Kinematic)	Long Base Lines	None
	Poor Satellite Constellation	None
	Poor Antenna Visibility	Reduce Visibility Mask
Relative Accuracy	Poor System Calibration	Recalibrate IMU and sensor offsets/settings
	Inaccurate System	None
Laser Noise	Poor Laser Timing	None
	Poor Laser Reception	None
	Poor Laser Power	None
	Irregular Laser Shape	None

### Operational measures taken to improve relative accuracy:

**Low Flight Altitude:** Terrain following is employed to maintain a constant above ground level (AGL). Laser horizontal errors are a function of flight altitude above ground (i.e.,  $\sim 1/3000^{\text{th}}$  AGL flight altitude).

**Focus Laser Power at narrow beam footprint:** A laser return must be received by the system above a power threshold to accurately record a measurement. The strength of the laser return is a function of laser emission power, laser footprint, flight altitude and the reflectivity of the target. While surface reflectivity cannot be controlled, laser power can be increased and low flight altitudes can be maintained.

**Reduced Scan Angle:** Edge-of-scan data can become inaccurate. The scan angle was reduced to a maximum of  $\pm 15^\circ$  from nadir, creating a narrow swath width and greatly reducing laser shadows from trees and buildings.

**Quality GPS:** Flights took place during optimal GPS conditions (e.g., 6 or more satellites and PDOP [Position Dilution of Precision] less than 3.0). Before each flight, the PDOP was determined for the survey day. During all flight times, a dual frequency DGPS base station recording at 1-second epochs was utilized and a maximum baseline length between the aircraft and the control points was less than 19 km (11.5 miles) at all times.

**Ground Survey:** Ground survey point accuracy (i.e.  $<1.5$  cm RMSE) occurs during optimal PDOP ranges and targets a minimal baseline distance of 4 miles between GPS rover and base. Robust statistics are, in part, a function of sample size (n) and distribution. Ground survey RTK points are distributed to the extent possible throughout multiple flight lines and across the survey area.

**50% Side-Lap (100% Overlap):** Overlapping areas are optimized for relative accuracy testing. Laser shadowing is minimized to help increase target acquisition from multiple scan angles. Ideally, with a 50% side-lap, the most nadir portion of one flight line coincides with the edge (least nadir) portion of overlapping flight lines. A minimum of 50% side-lap with terrain-followed acquisition prevents data gaps.

**Opposing Flight Lines:** All overlapping flight lines are opposing. Pitch, roll and heading errors are amplified by a factor of two relative to the adjacent flight line(s), making misalignments easier to detect and resolve.

**Native (First Return) Point Densities by AOI:**

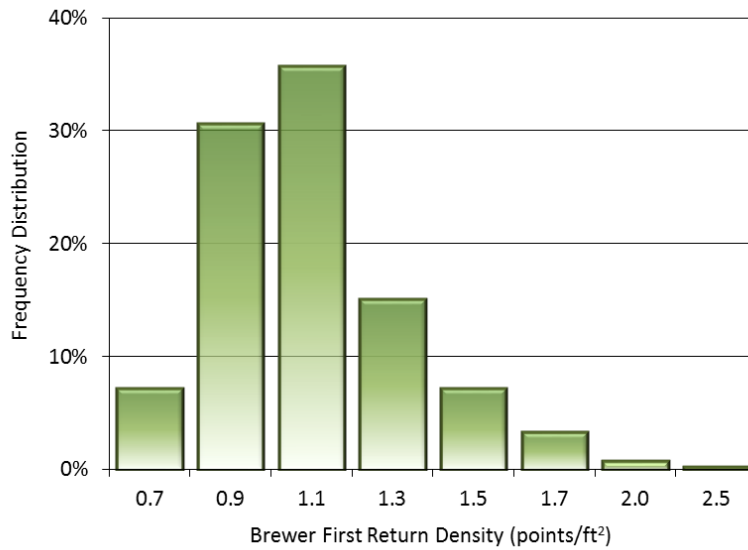


**Figure 12: Frequency distribution of first return densities (native densities) of the Brewer study area**

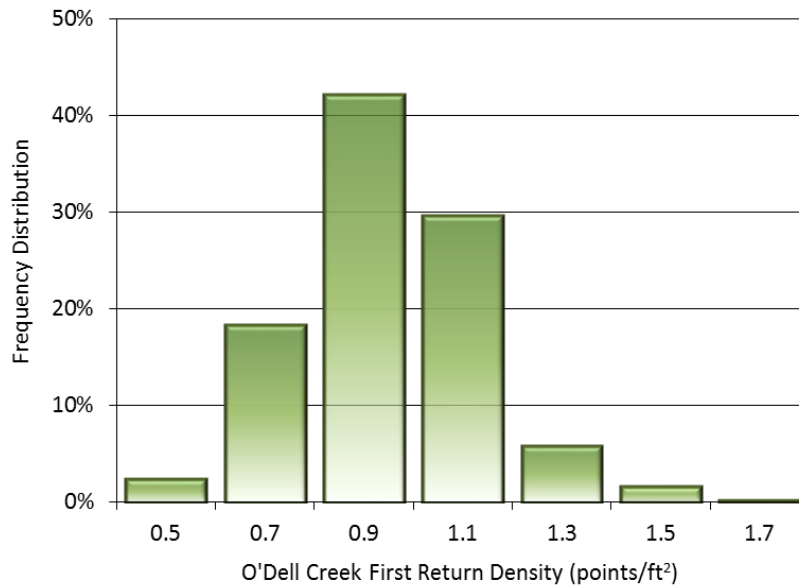


**Figure 13: Frequency distribution of first return densities (native densities) of the O'Dell Creek study area**

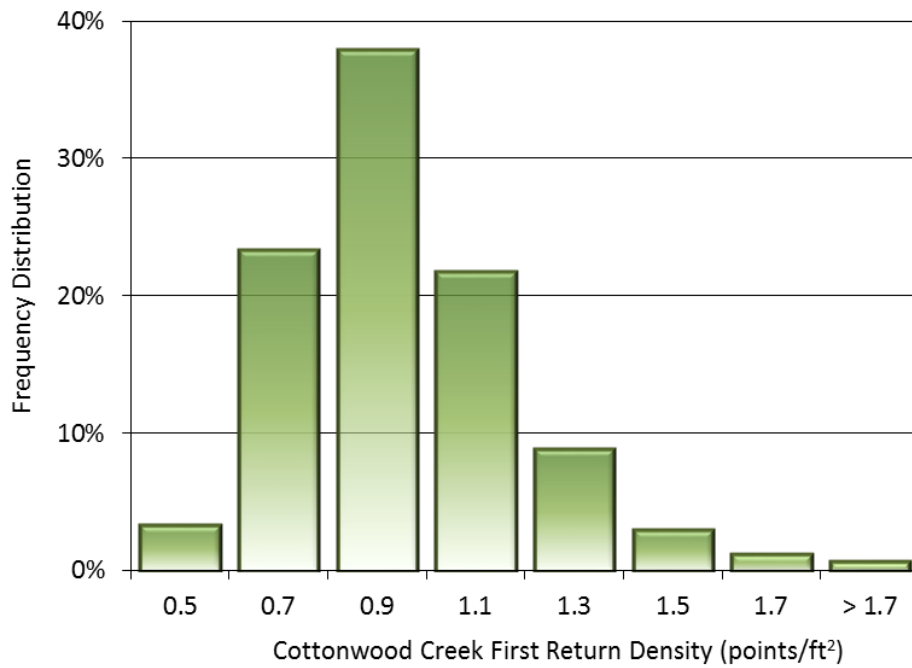


**Figure 14: Frequency distribution of first return densities (native densities) of the Cottonwood Creek study area**

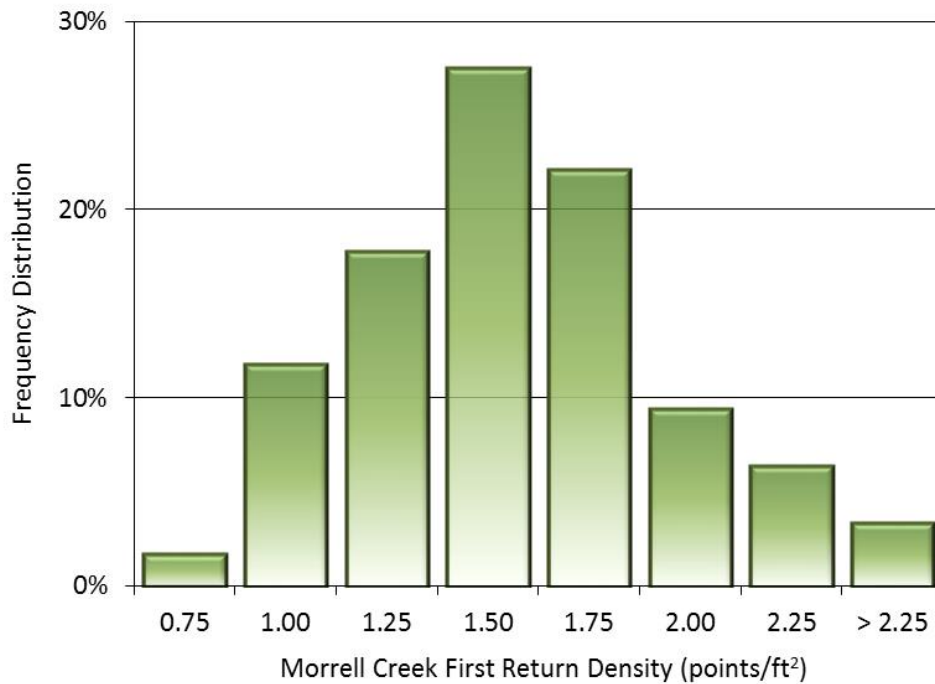


**Figure 15: Frequency distribution of first return densities (native densities) of the Morrell Creek study area**

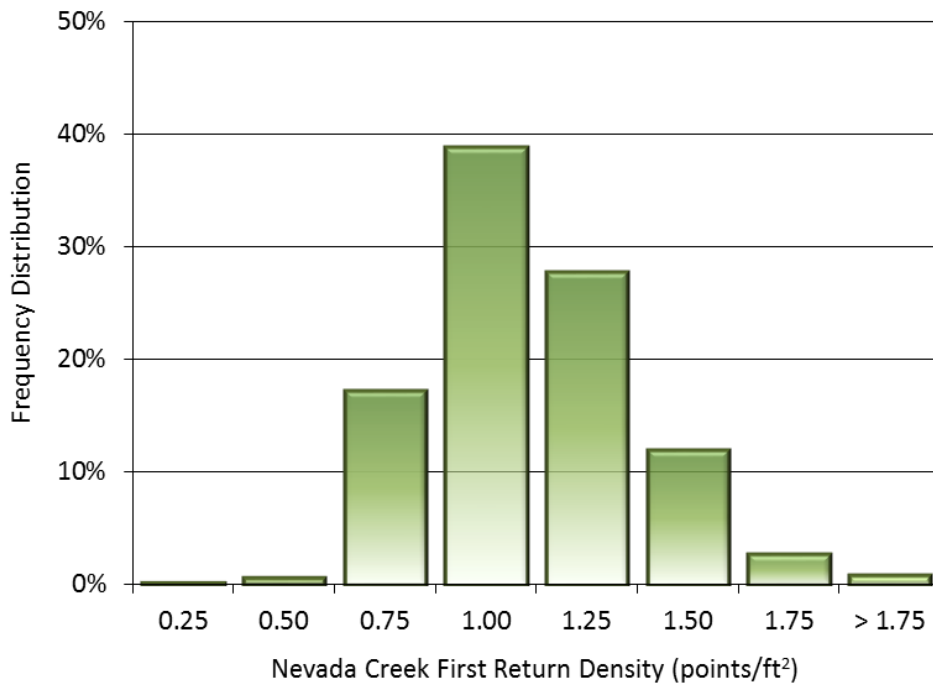


**Figure 16: : Frequency distribution of first return densities (native densities) of the Nevada Creek study area**

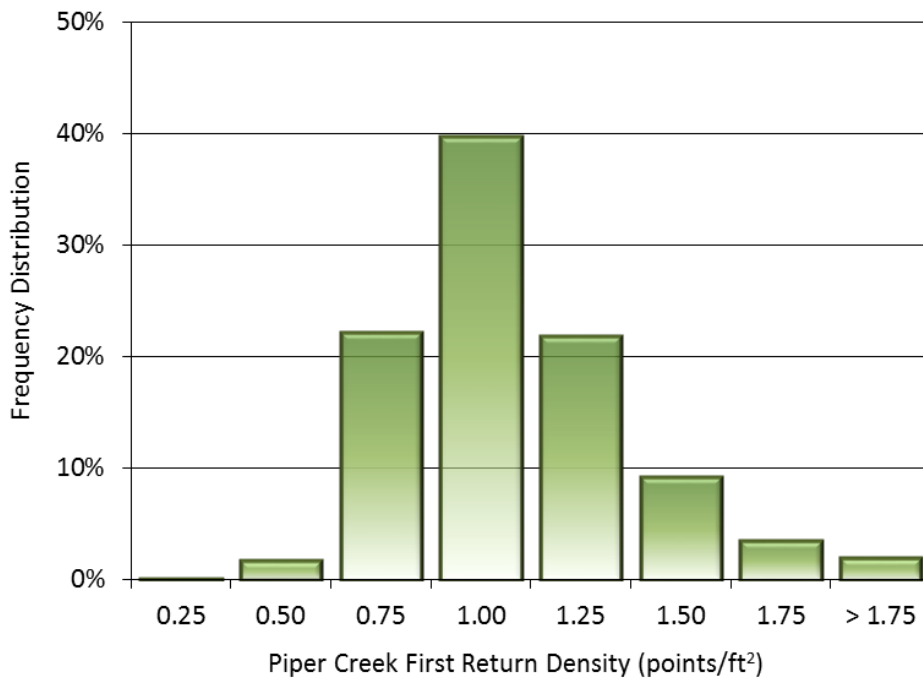


**Figure 17: Frequency distribution of first return densities (native densities) of the Piper Creek study area**

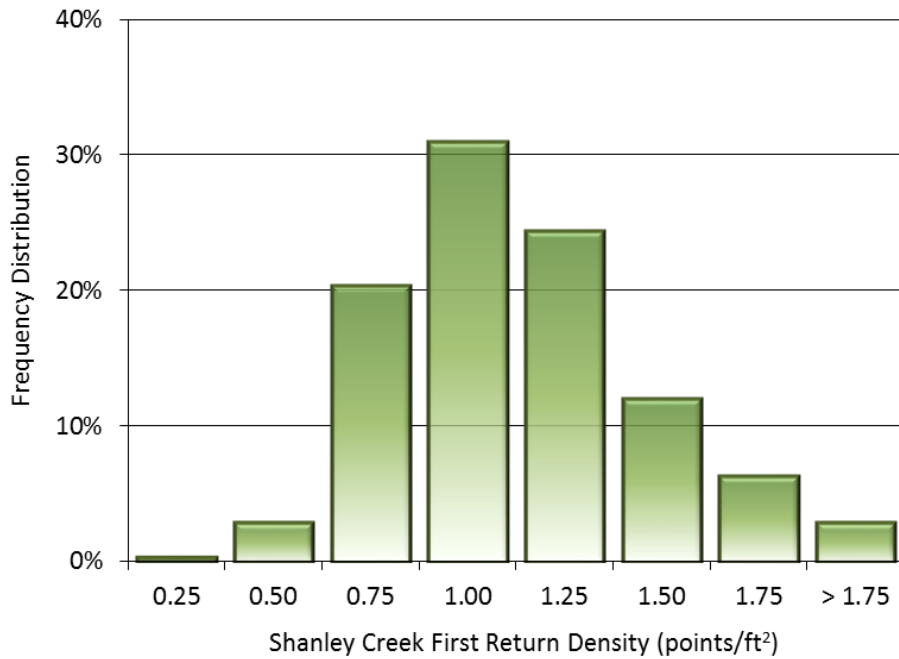


**Figure 18: Frequency distribution of first return densities (native densities) of the Shanley Creek study area**

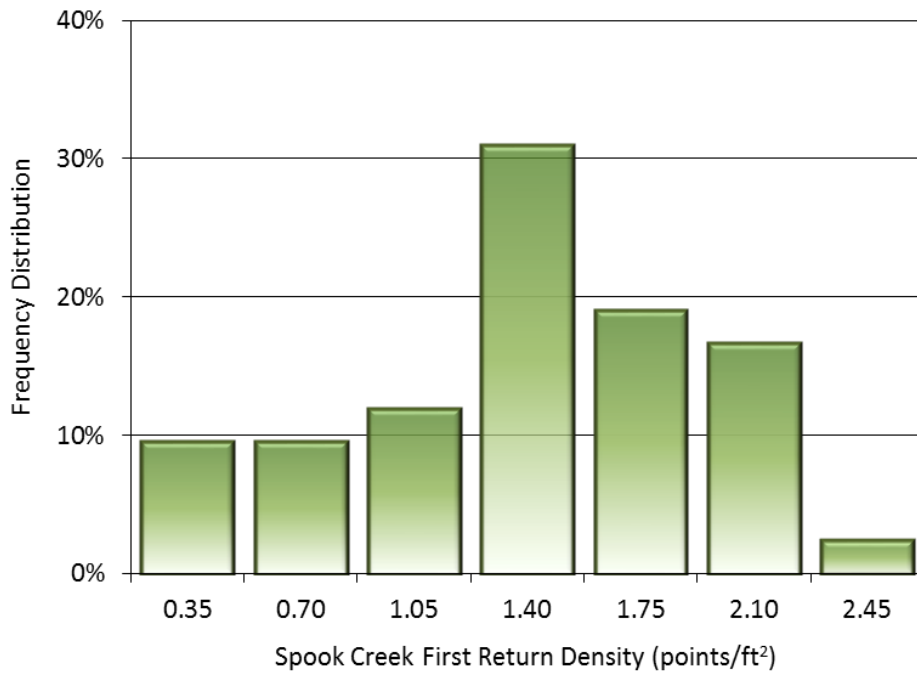


**Figure 19: Frequency distribution of first return densities (native densities) of the Spook Creek study area**

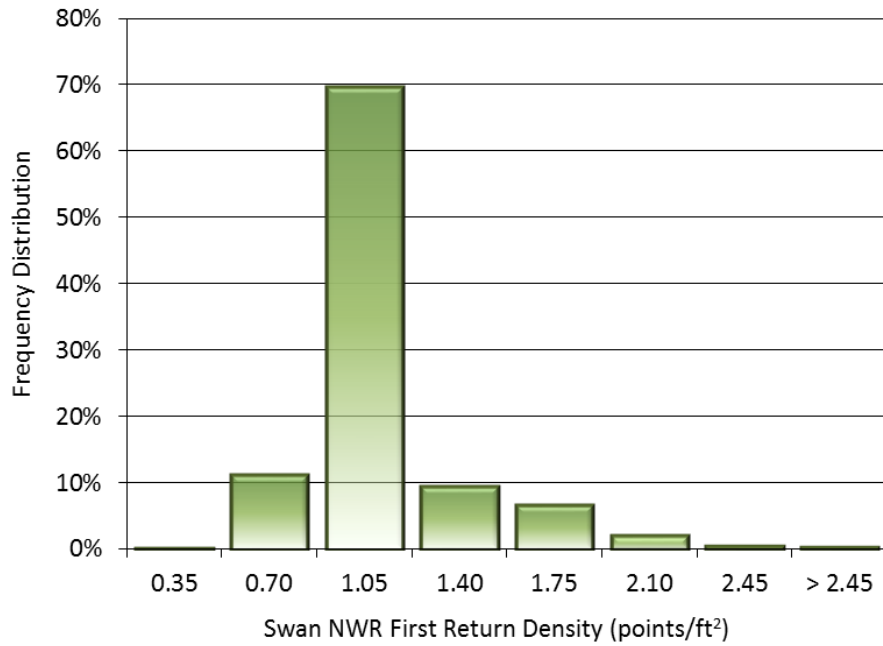


**Figure 20: Frequency distribution of first return densities (native densities) of the Swan NWR study area**

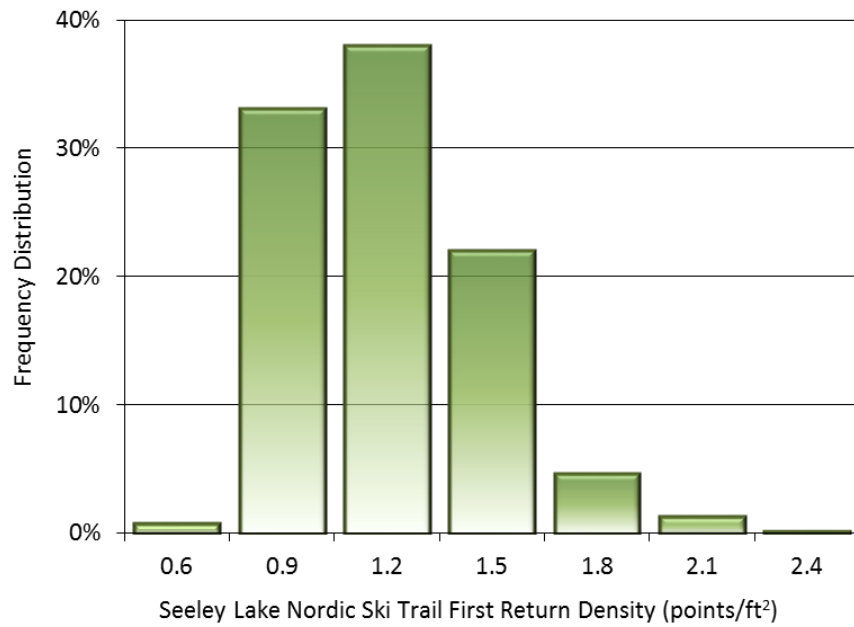


**Figure 21: Frequency distribution of first return densities (native densities) of the Seeley Lake Nordic Ski Trail study area**

**Ground Point Densities by AOI:**

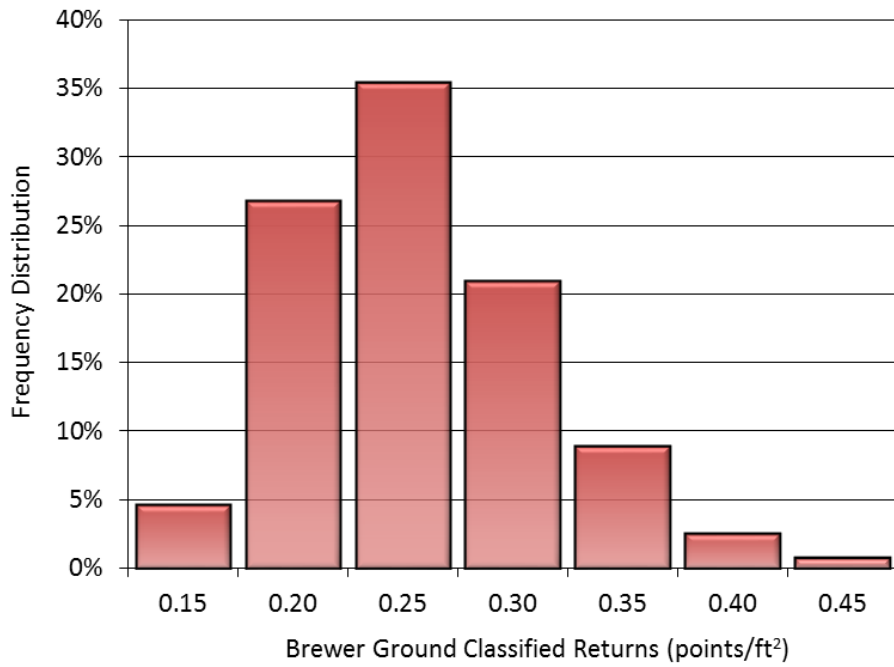


**Figure 22: Frequency distribution of ground return densities of the Brewer study area**

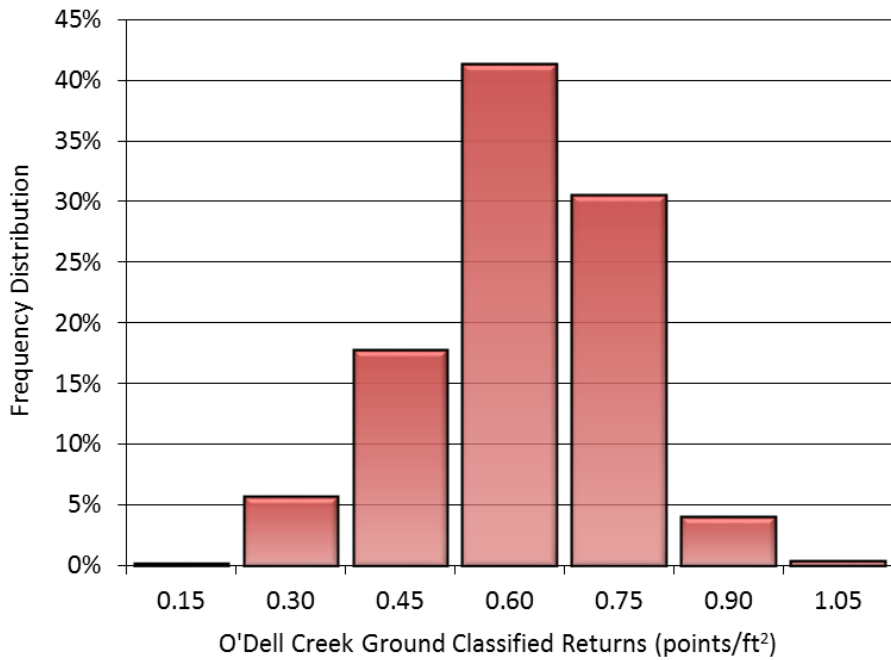


**Figure 23: Frequency distribution of ground return densities of the O'Dell Creek study area**

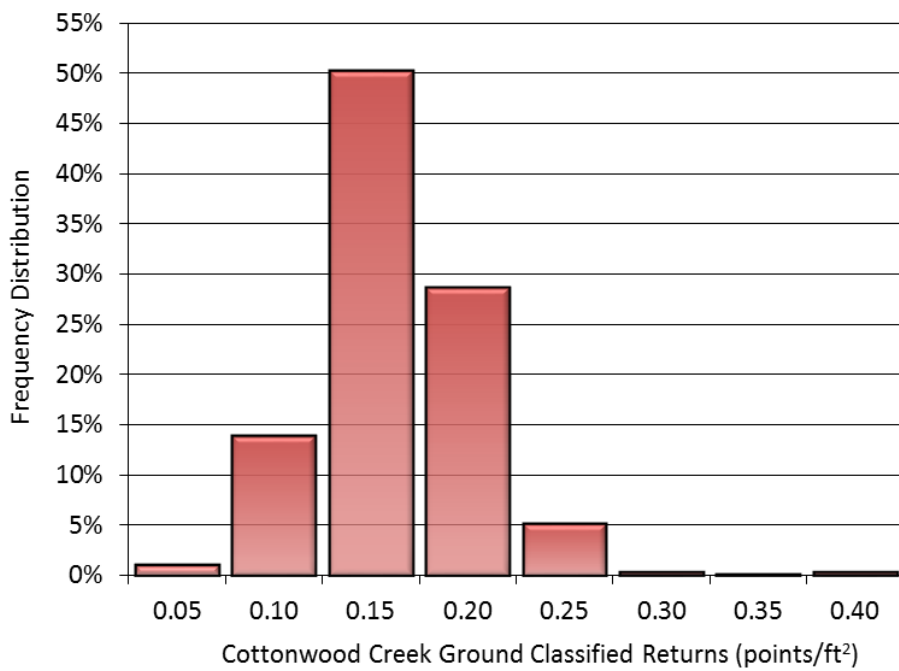


**Figure 24: Frequency distribution of ground return densities of the Cottonwood Creek study area**

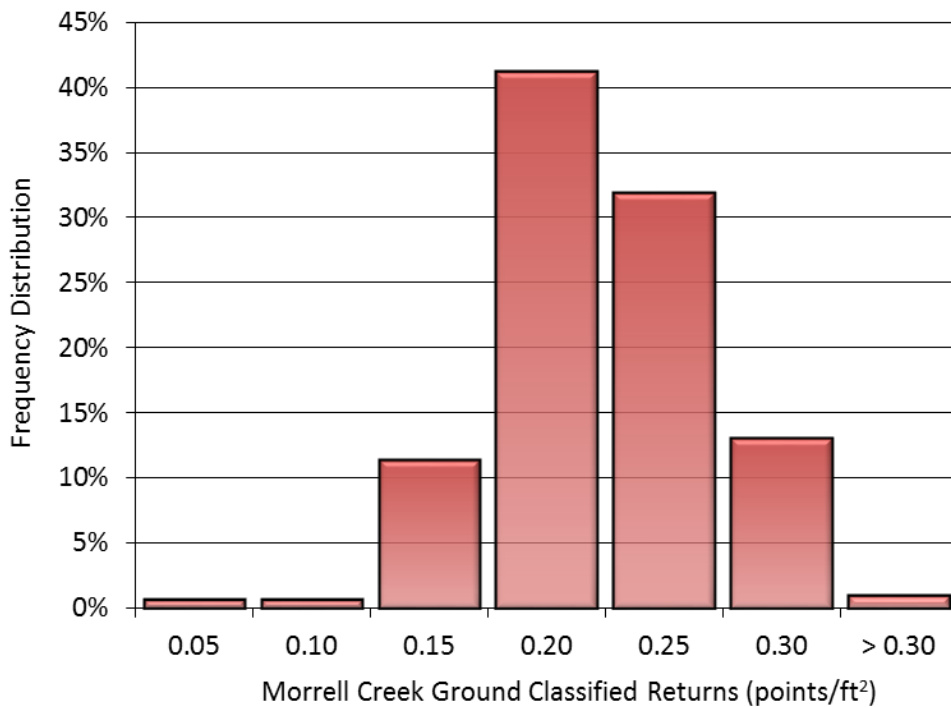


**Figure 25: Frequency distribution of ground return densities of the Morrell Creek study area**

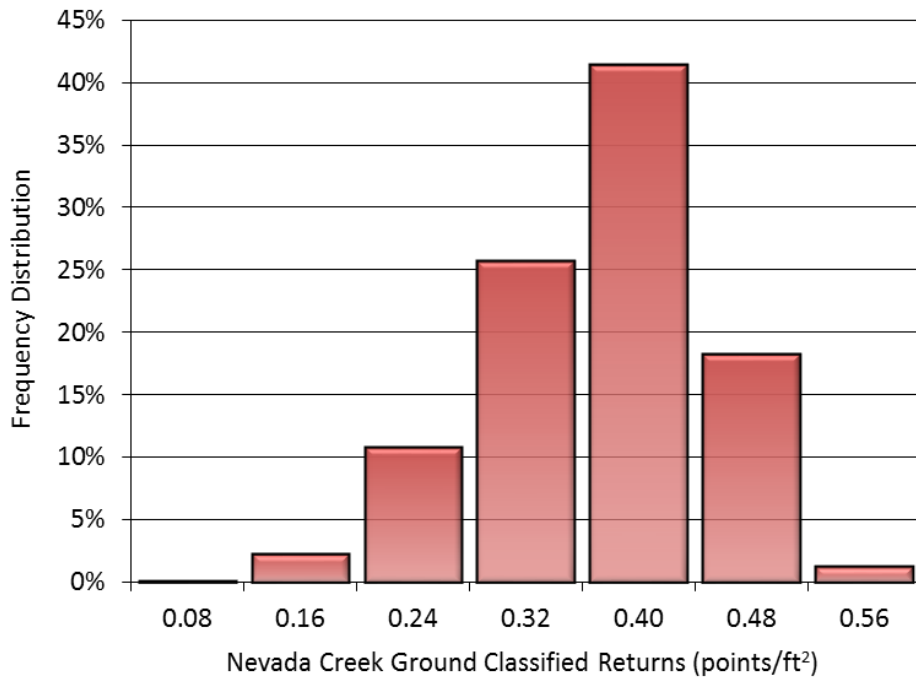


**Figure 26: Frequency distribution of ground return densities of the Nevada Creek study area**

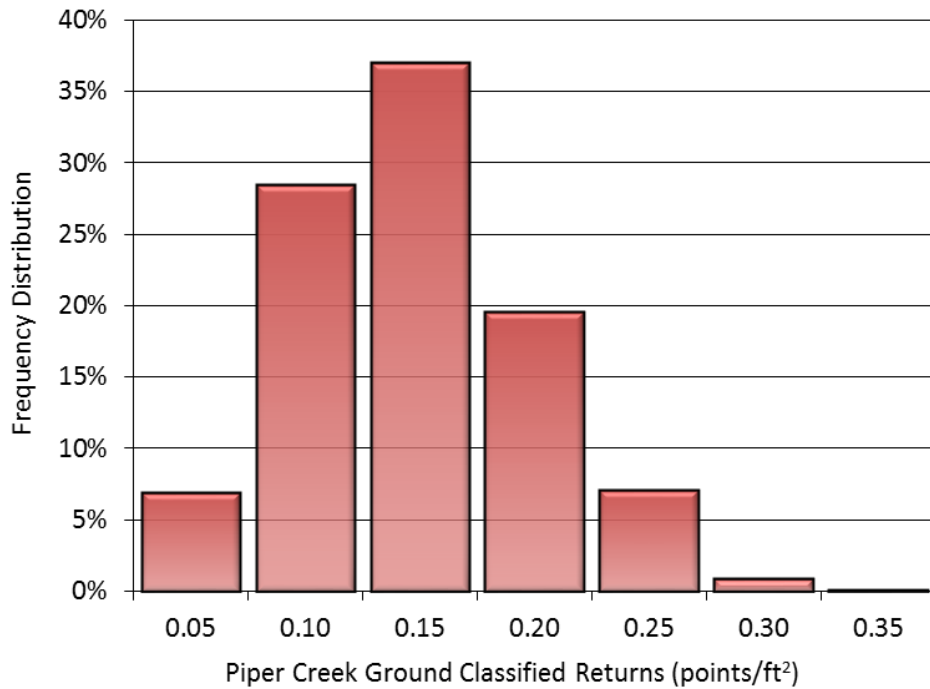


**Figure 27: Frequency distribution of ground return densities of the Piper Creek study area**

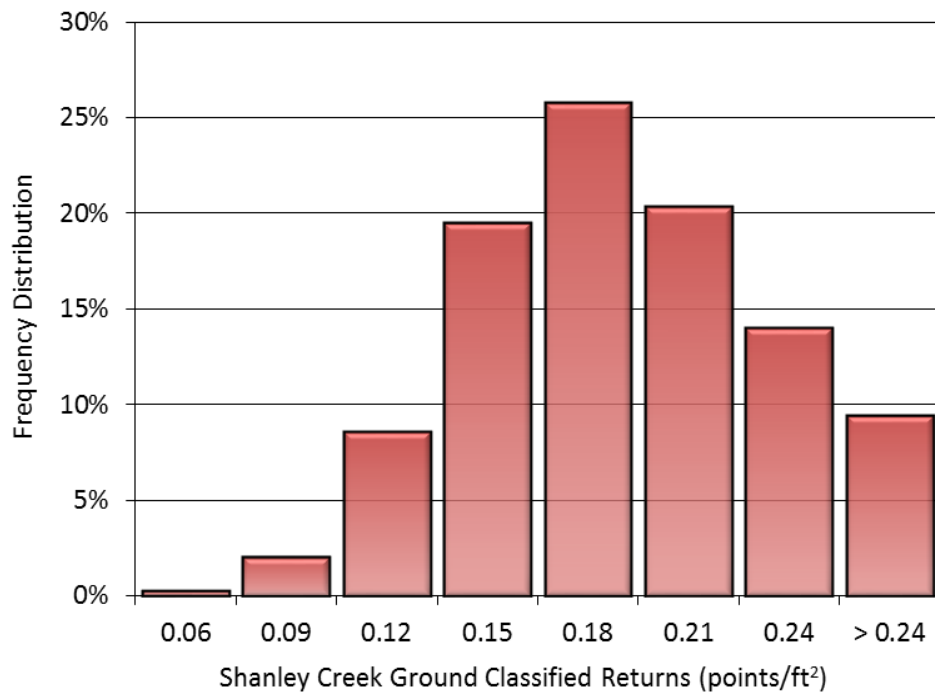


**Figure 28: Frequency distribution of ground return densities of the Shanley Creek study area**

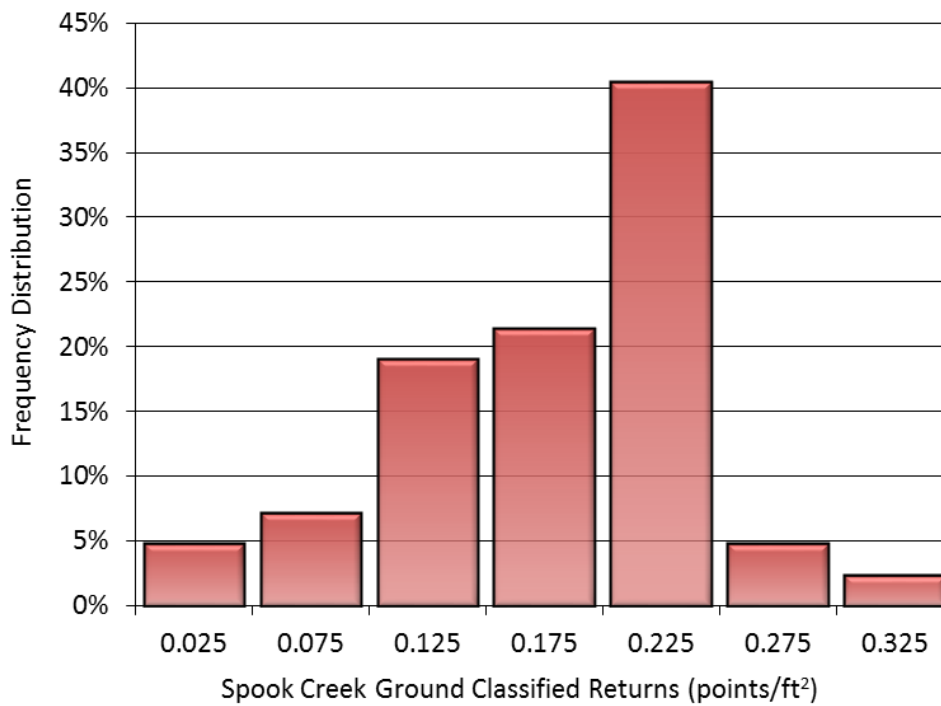


**Figure 29: Frequency distribution of ground return densities of the Spook Creek study area**

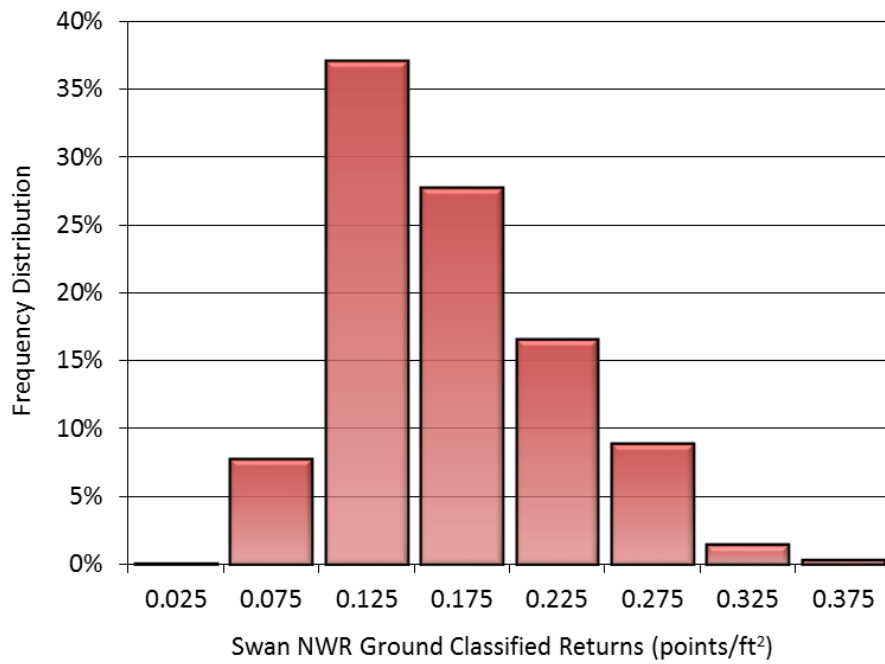


**Figure 30: Frequency distribution of ground return densities of the Swan NWR study area**

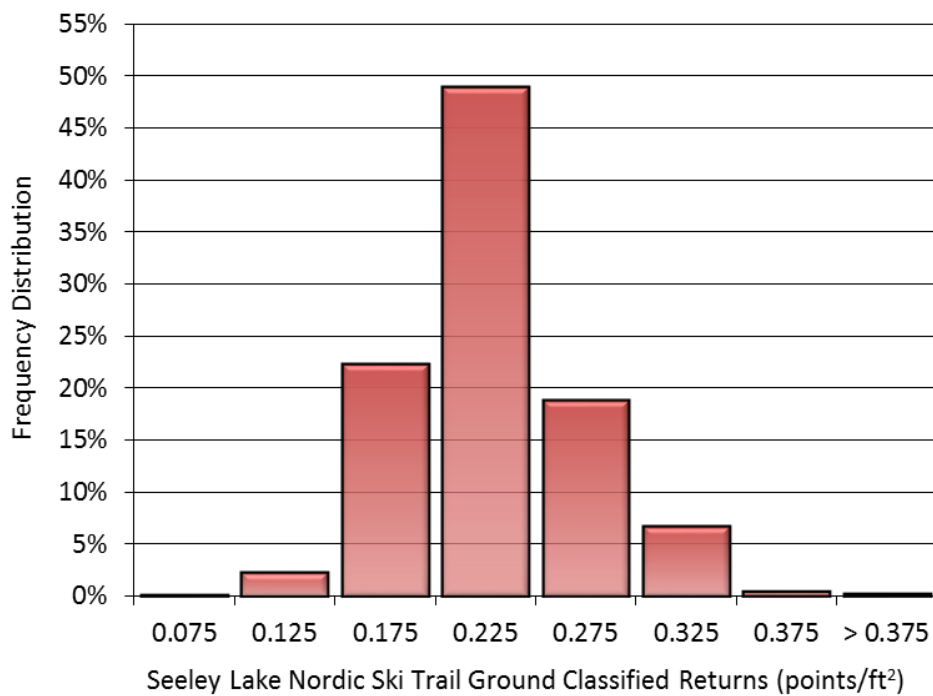


**Figure 31: Frequency distribution of ground return densities of the Seeley Lake Nordic Ski Trail study area**

**Absolute Accuracies by AOI:**

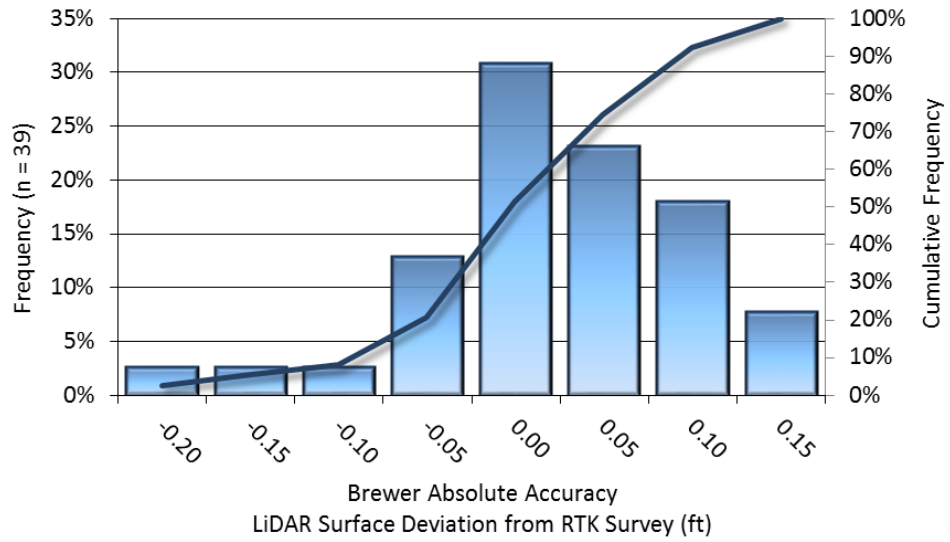


**Figure 32: Frequency histogram for the Brewer AOI LiDAR surface deviation from RTK values**

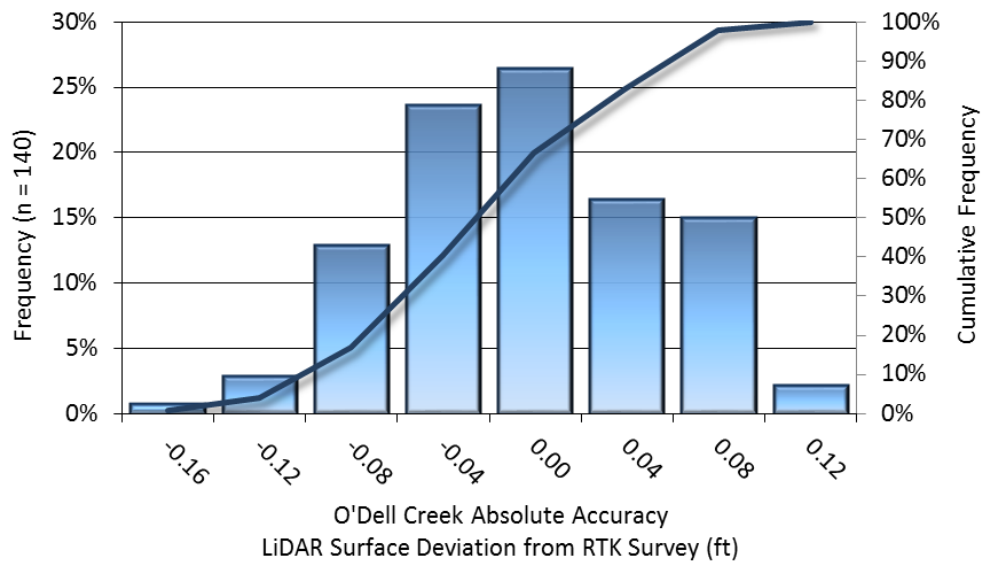


**Figure 33: Frequency histogram for the O'Dell Creek AOI LiDAR surface deviation from RTK values**

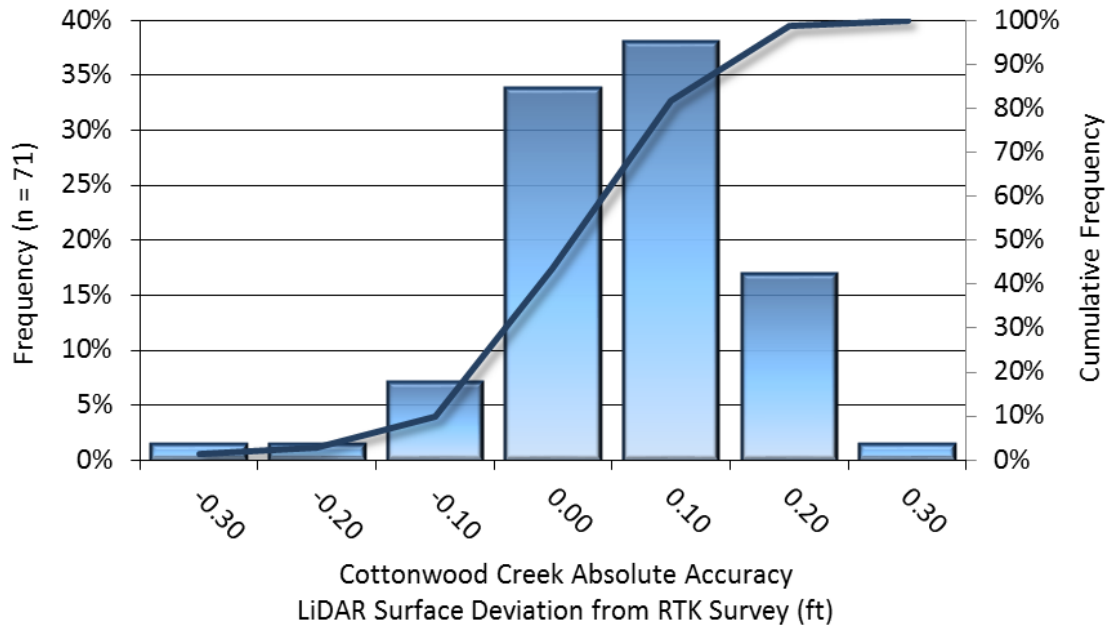


Figure 34: Frequency histogram for the Cottonwood Creek AOI LiDAR surface deviation from RTK values

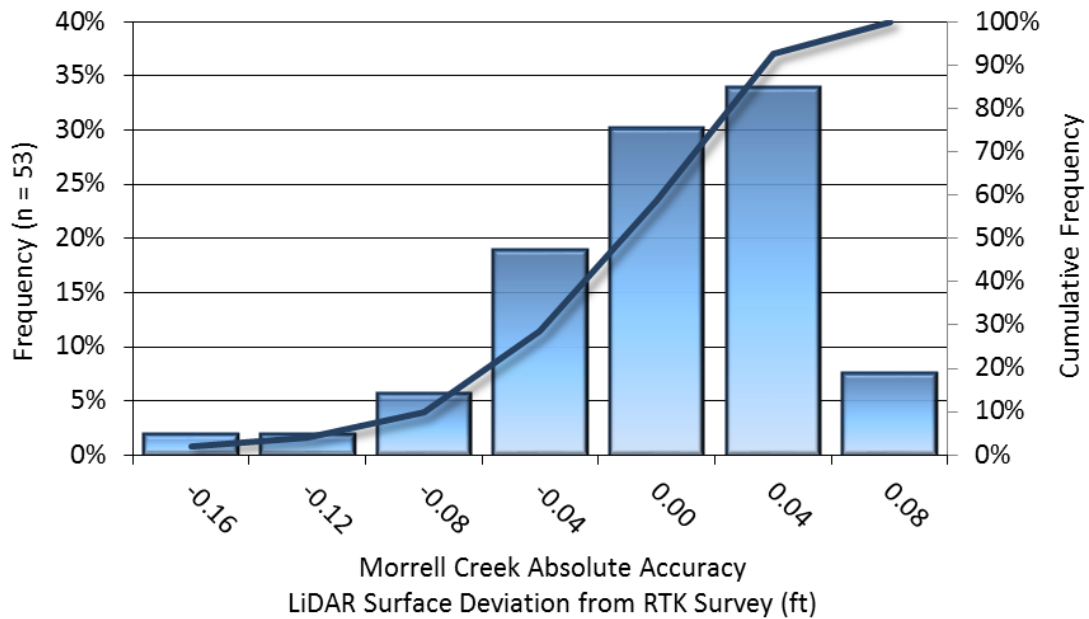


Figure 35: Frequency histogram for the Cottonwood Creek AOI LiDAR surface deviation from RTK values

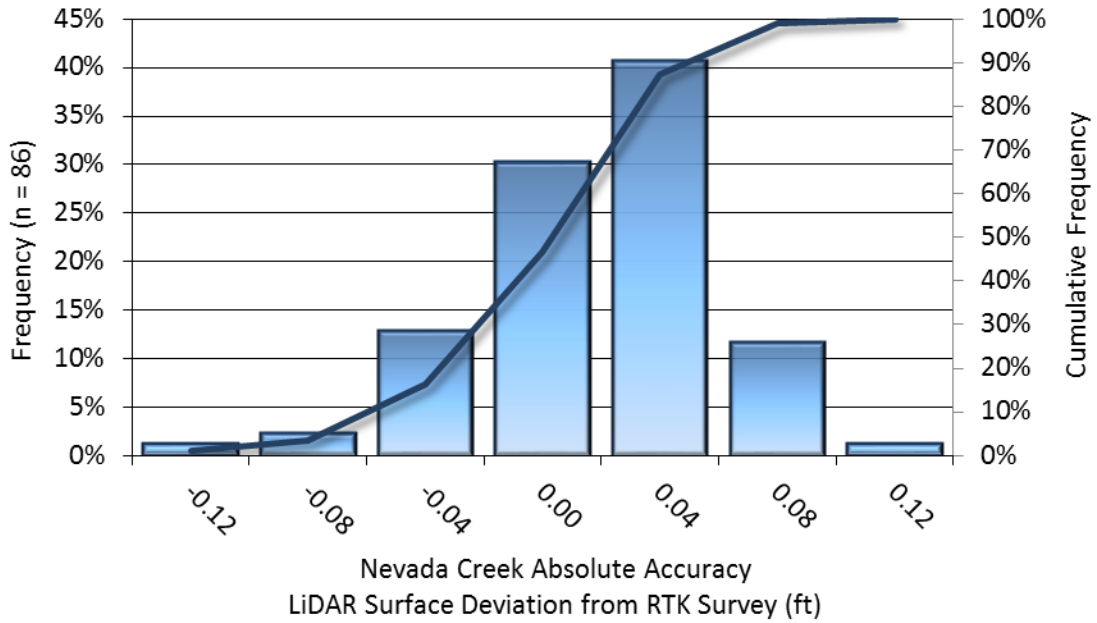


Figure 36: Frequency histogram for the Nevada Creek AOI LiDAR surface deviation from RTK values

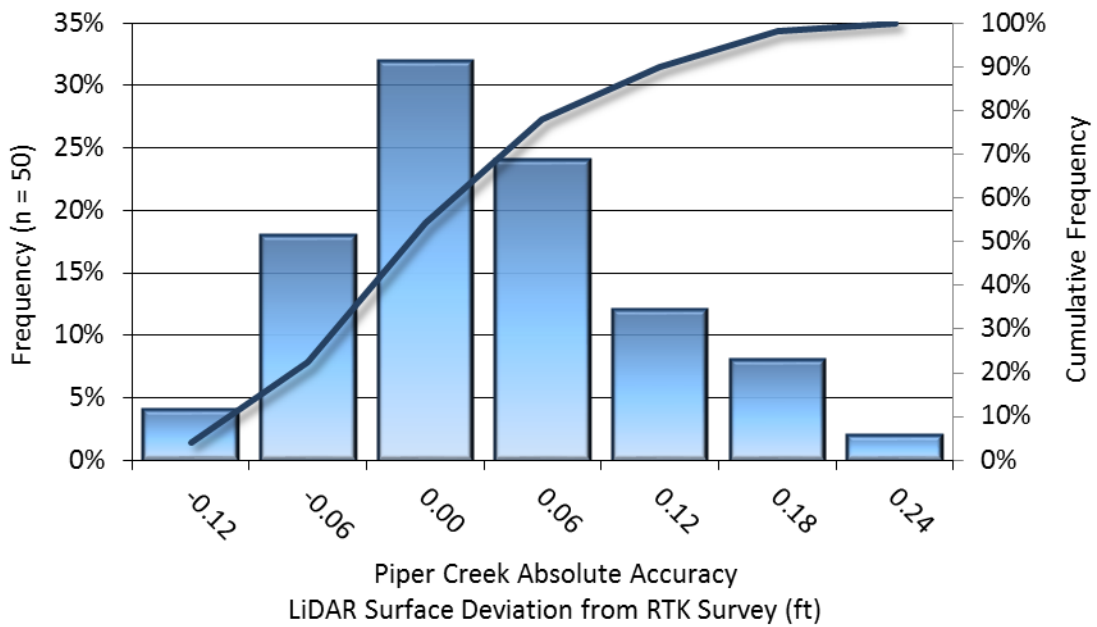
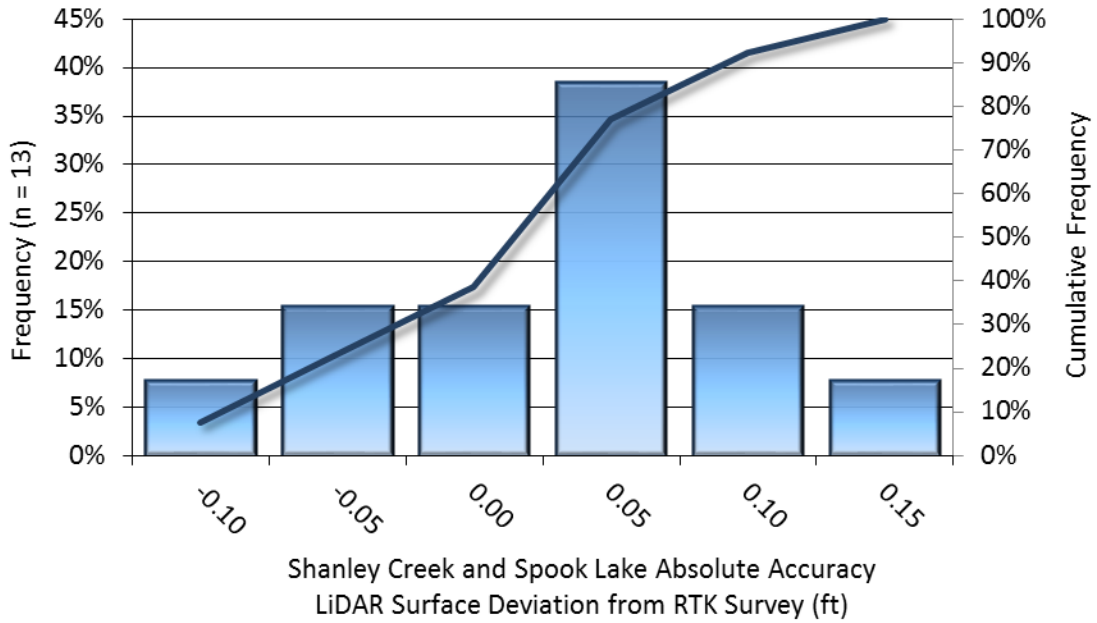
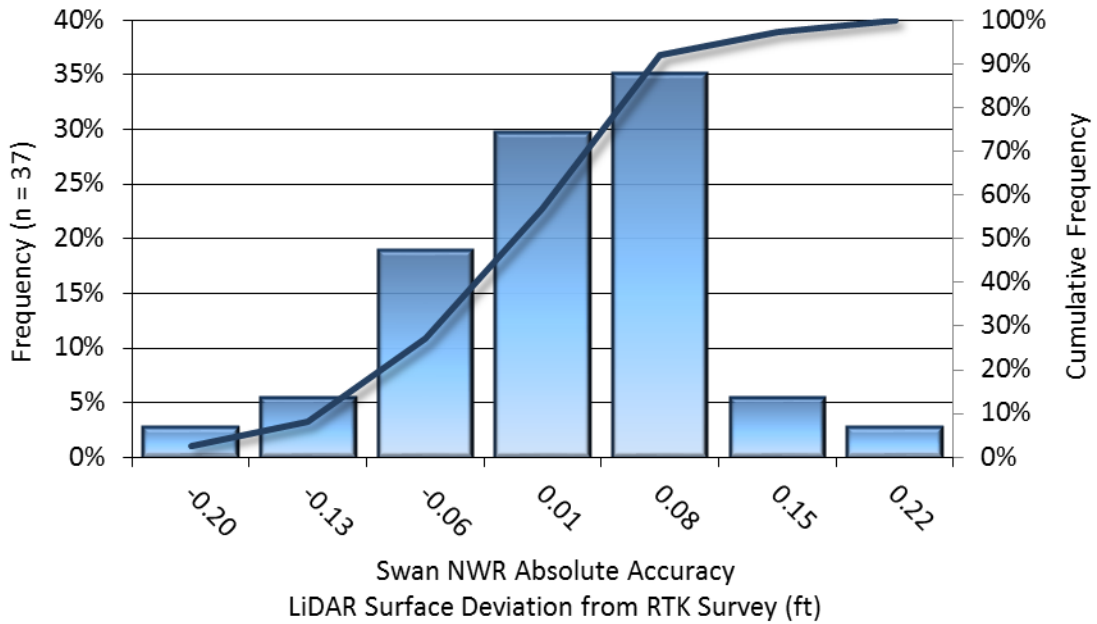


Figure 37: Frequency histogram for the Piper Creek AOI LiDAR surface deviation from RTK values



**Figure 38: Frequency histogram for the Shanley Creek and Spook Lake AOIs LiDAR surface deviation from RTK values**



**Figure 39: Frequency histogram for the Swan NWR AOI LiDAR surface deviation from RTK values**

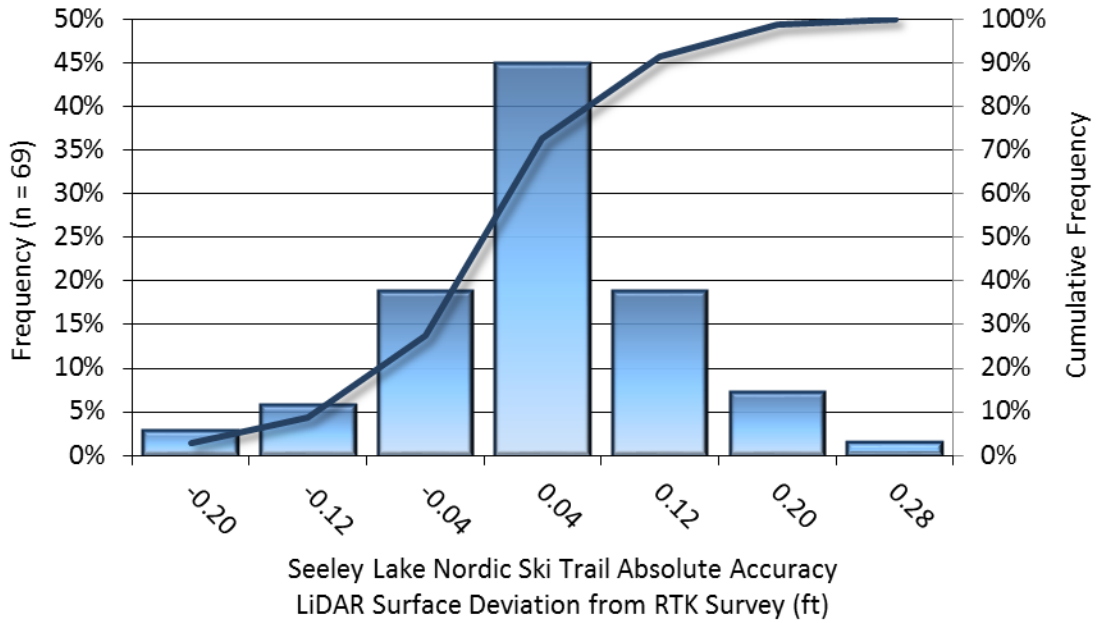


Figure 40: Frequency histogram for the Seeley Lake Nordic Ski Trail AOI LiDAR surface deviation from RTK values

**Vertical Relative Accuracies by AOI:**

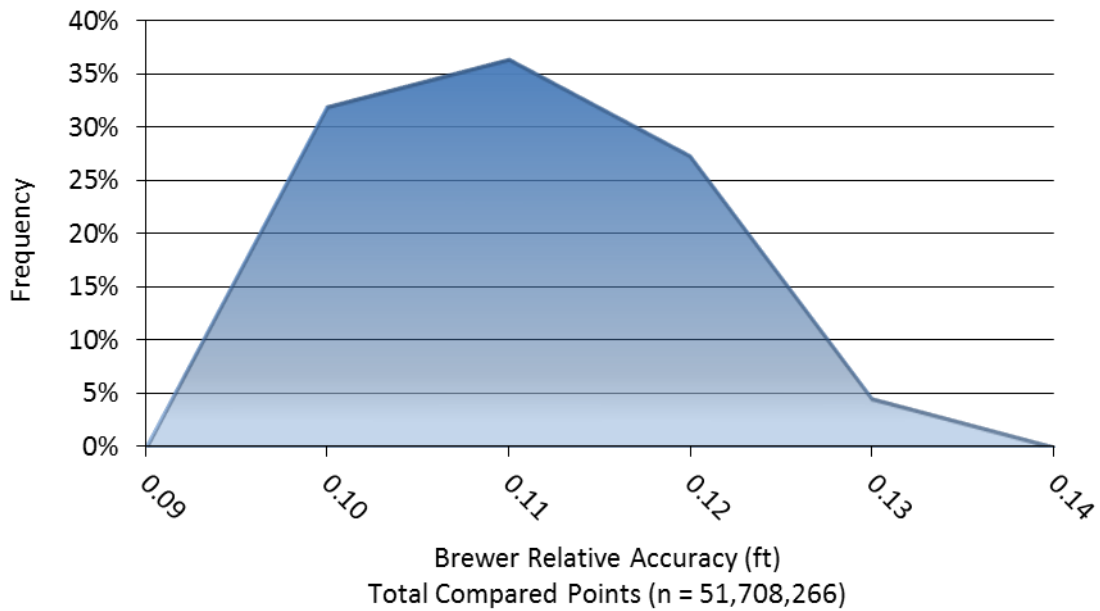


Figure 41: Frequency plot for relative vertical accuracy between flight lines in the Brewer AOI

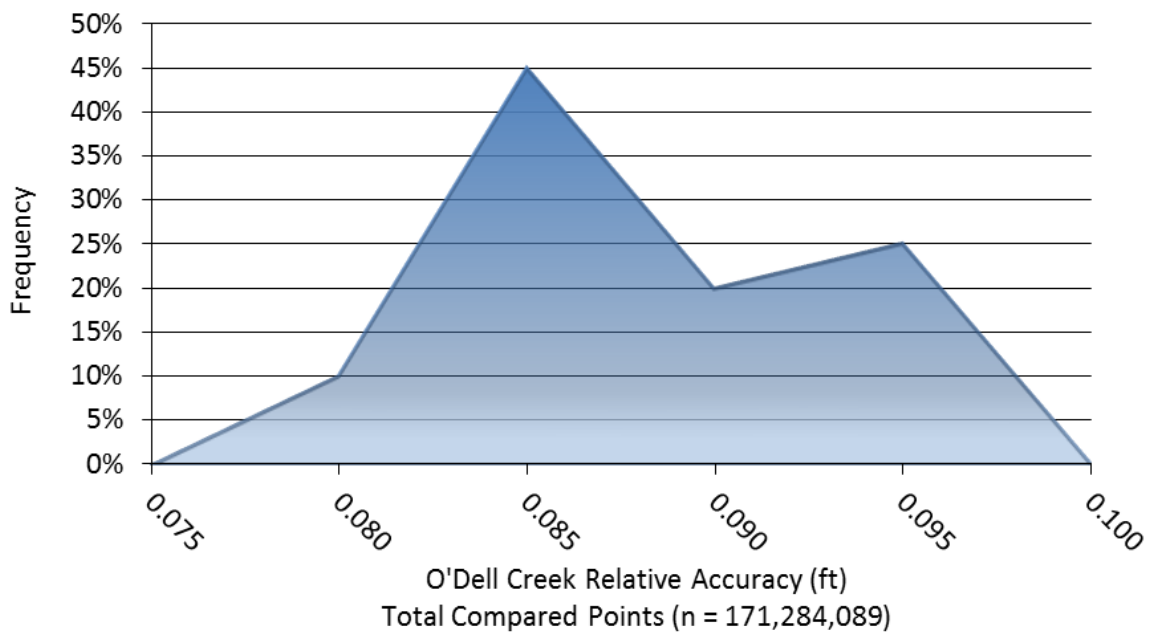


Figure 42: Frequency plot for relative vertical accuracy between flight lines in the O'Dell Creek AOI

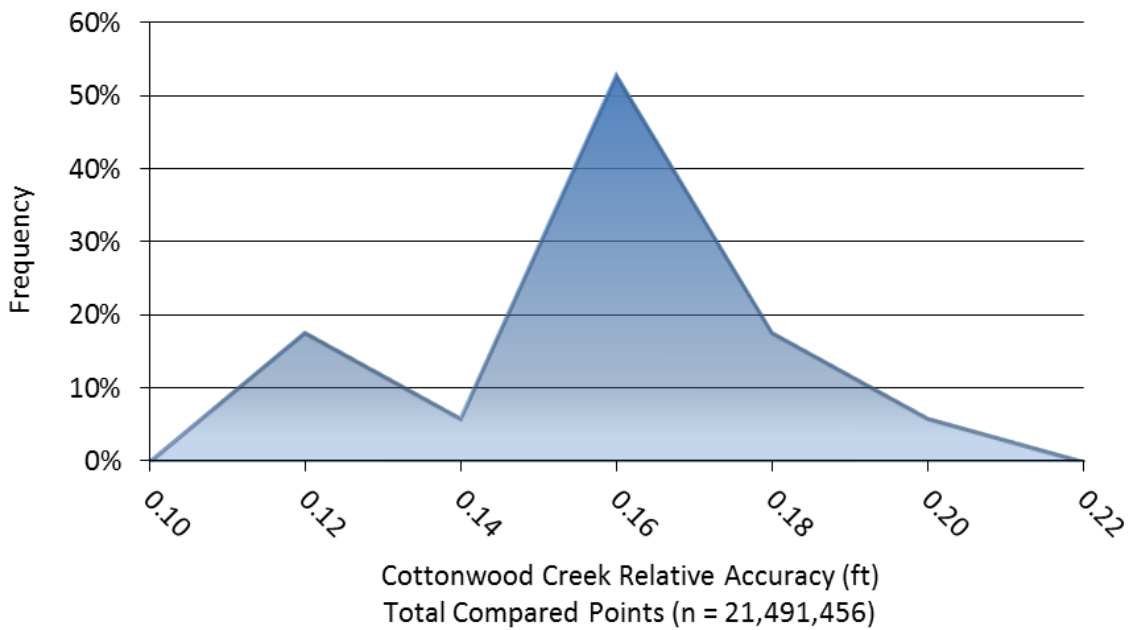


Figure 43: Frequency plot for relative vertical accuracy between flight lines in the Cottonwood Creek AOI

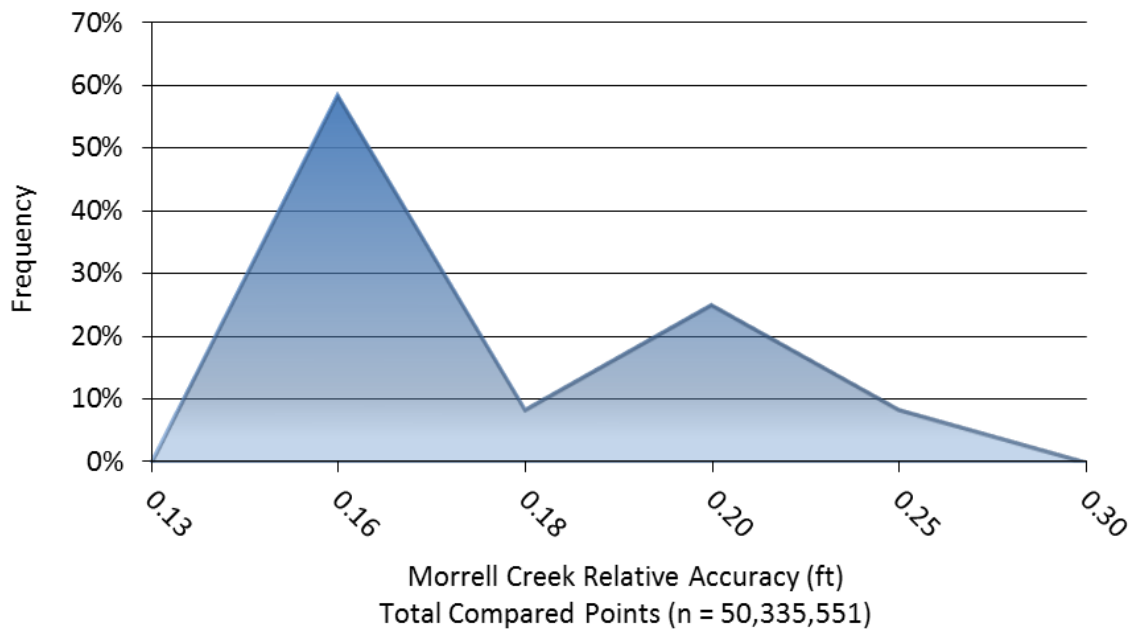


Figure 44: Frequency plot for relative vertical accuracy between flight lines in the Morrell Creek AOI

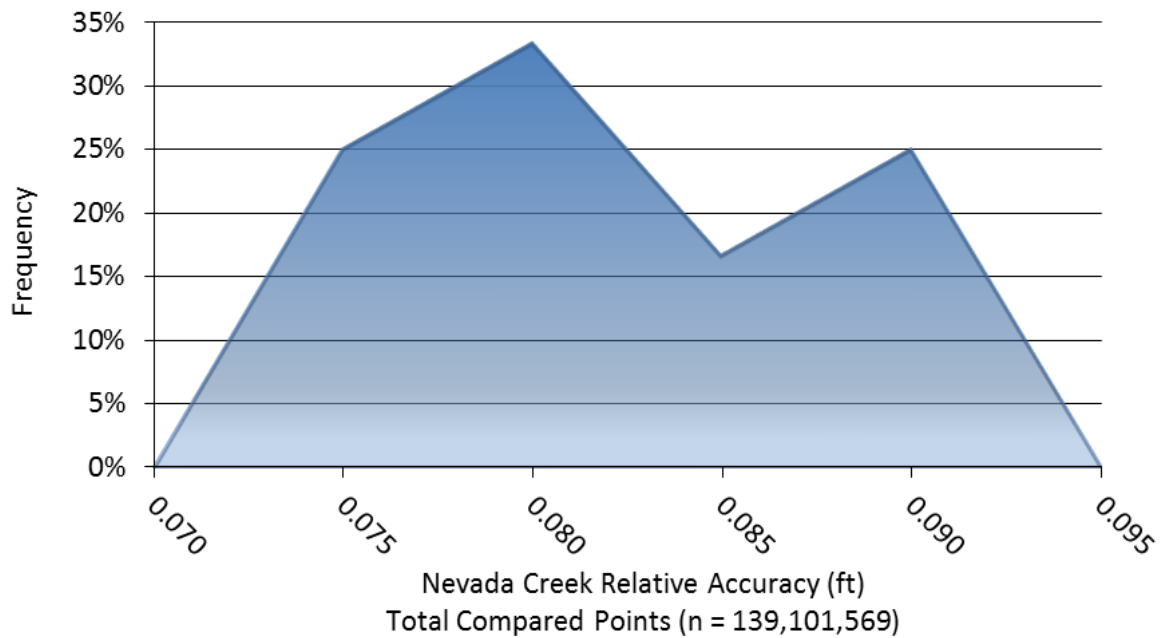


Figure 45: Frequency plot for relative vertical accuracy between flight lines in the Nevada Creek AOI

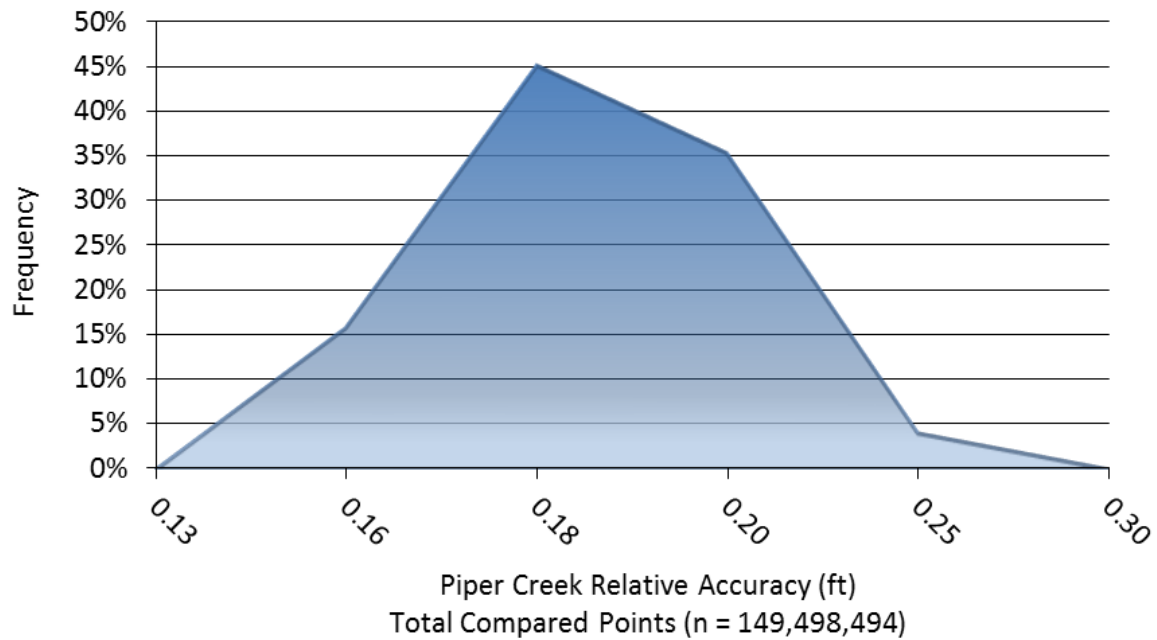


Figure 46: Frequency plot for relative vertical accuracy between flight lines in the Piper Creek AOI

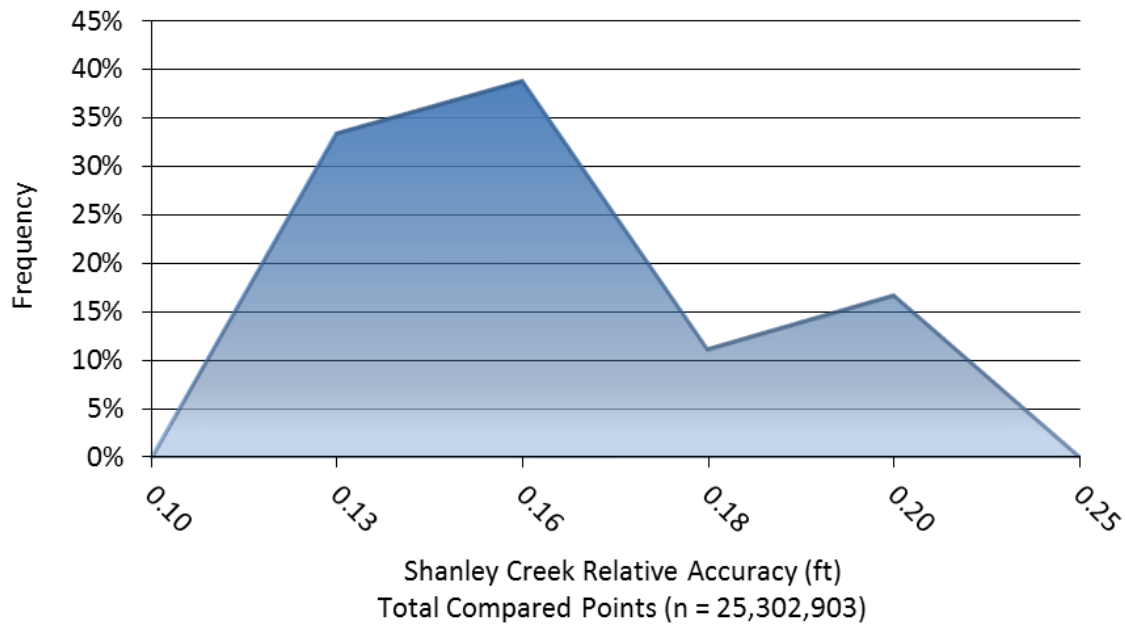
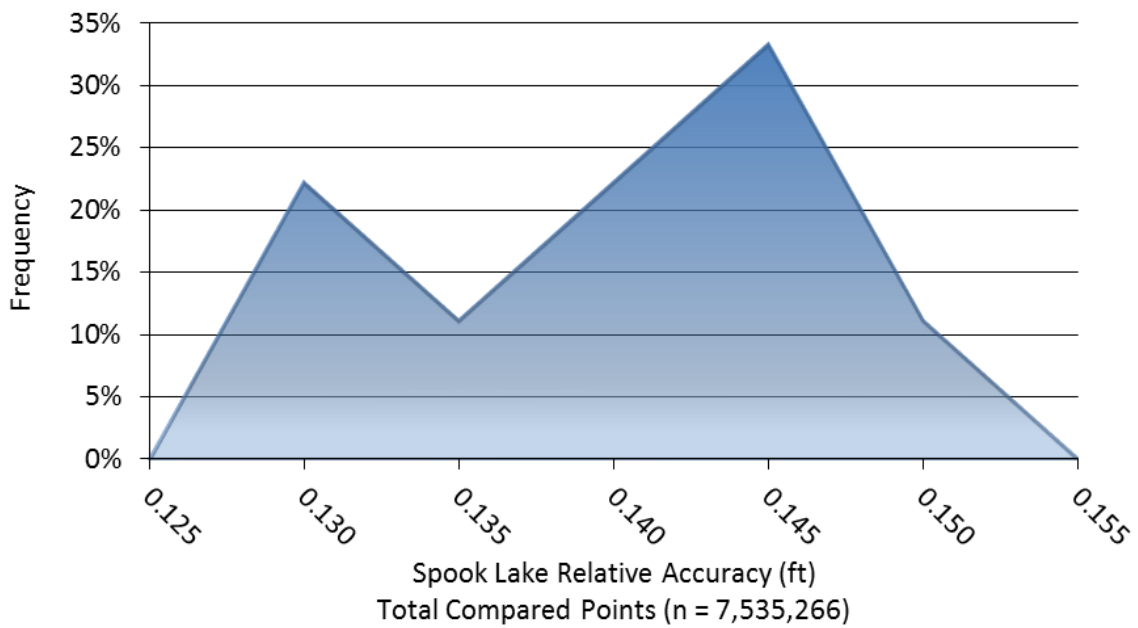
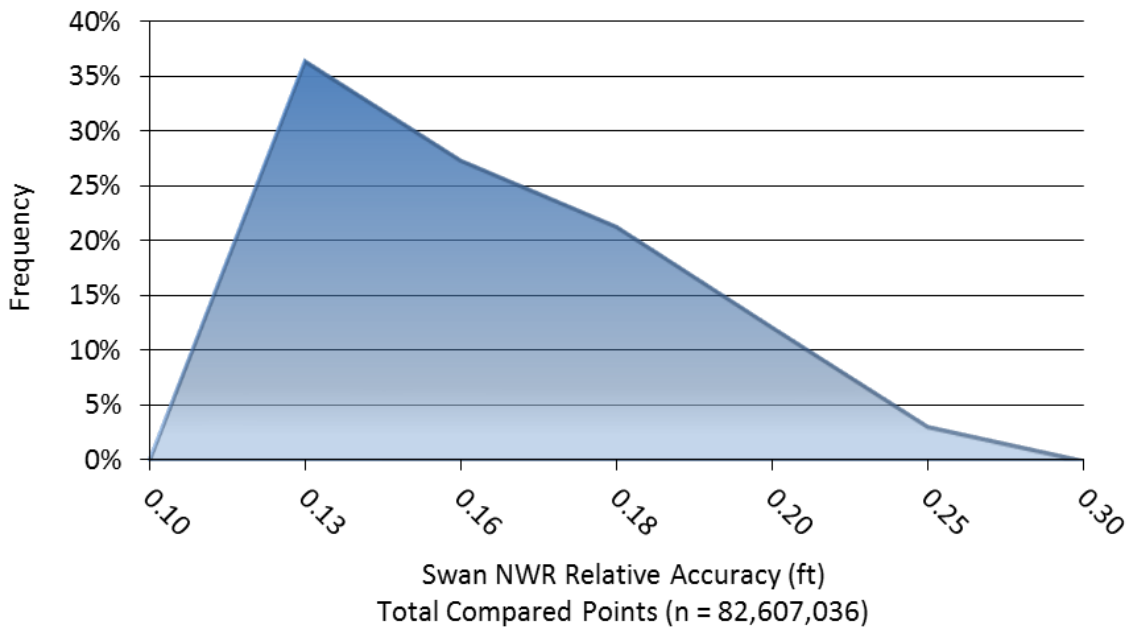


Figure 47: Frequency plot for relative vertical accuracy between flight lines in the Shanley Creek AOI



**Figure 48: Frequency plot for relative vertical accuracy between flight lines in the Spook Lake Creek AOI**



**Figure 49: Frequency plot for relative vertical accuracy between flight lines in the Swan NWR AOI**

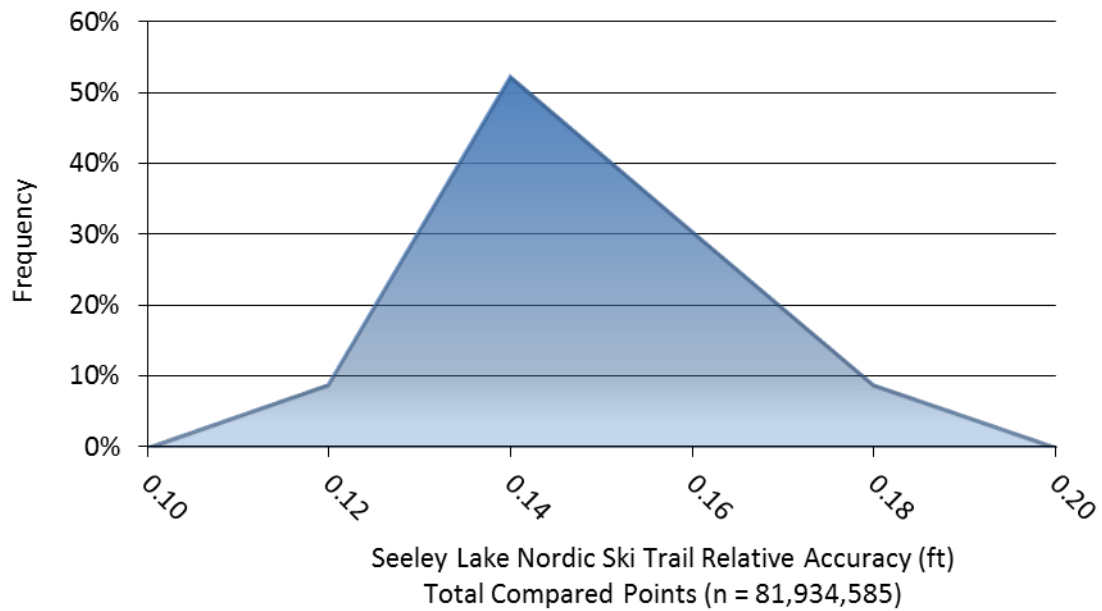


**Figure 50: Frequency plot for relative vertical accuracy between flight lines in the Seeley Lake Nordic Ski Trail AOI**

**Absolute Accuracies of Land Cover Class RTK checkpoints by AOI:**

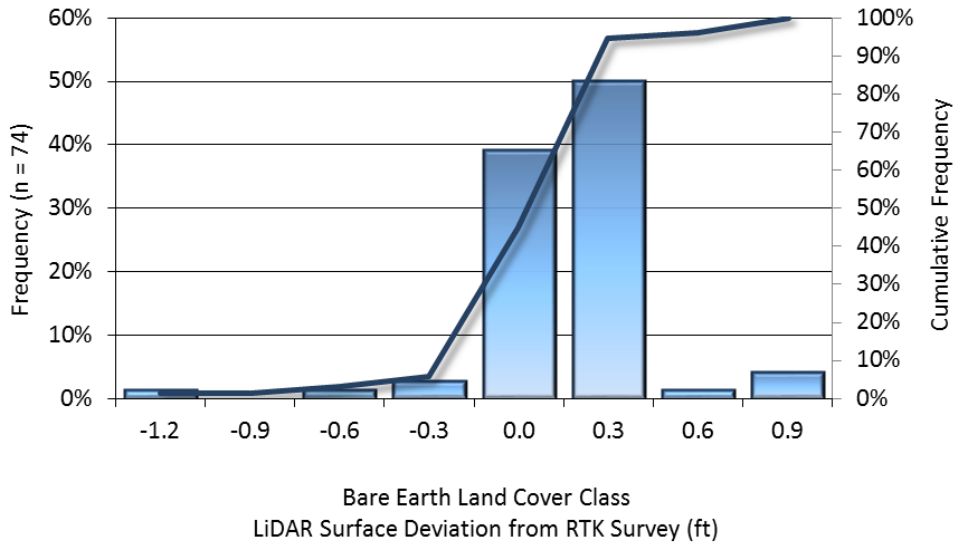


**Figure 51: Frequency histogram for LiDAR surface deviation from Bare Earth Landclass RTK values**

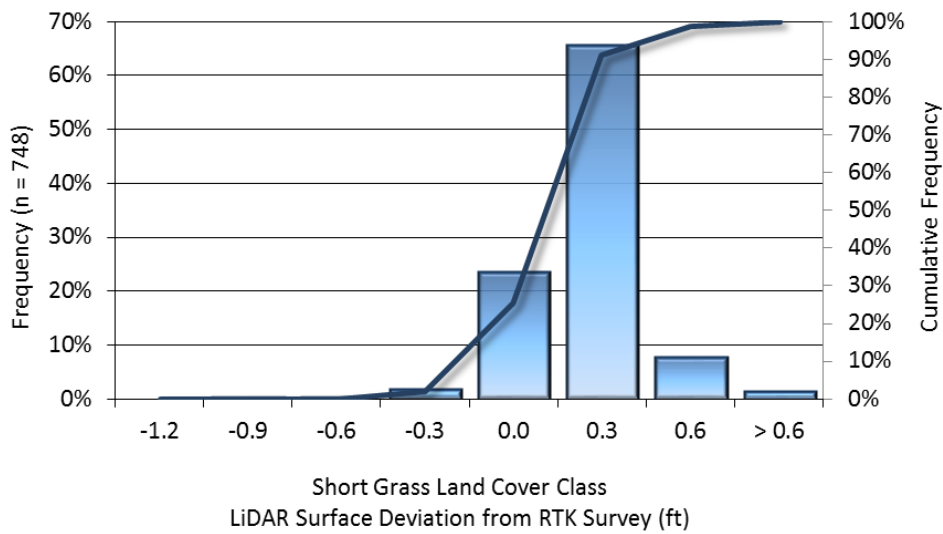


**Figure 52: Frequency histogram for LiDAR surface deviation from Short Grass Landclass RTK values**

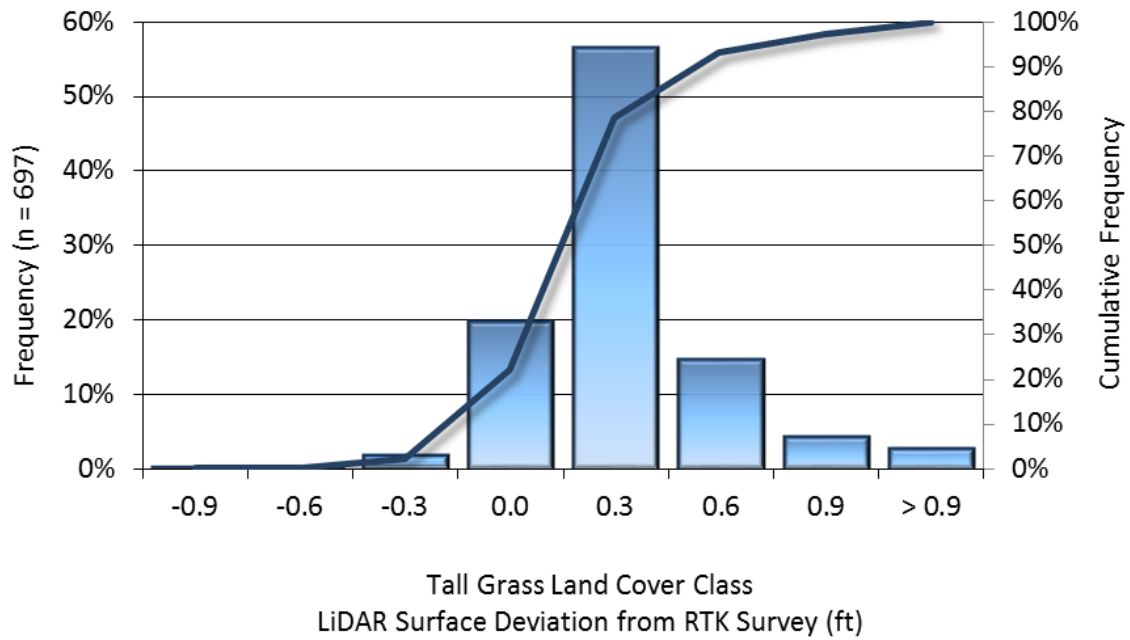


Figure 53: Frequency histogram for LiDAR surface deviation from Tall Grass Landclass RTK values

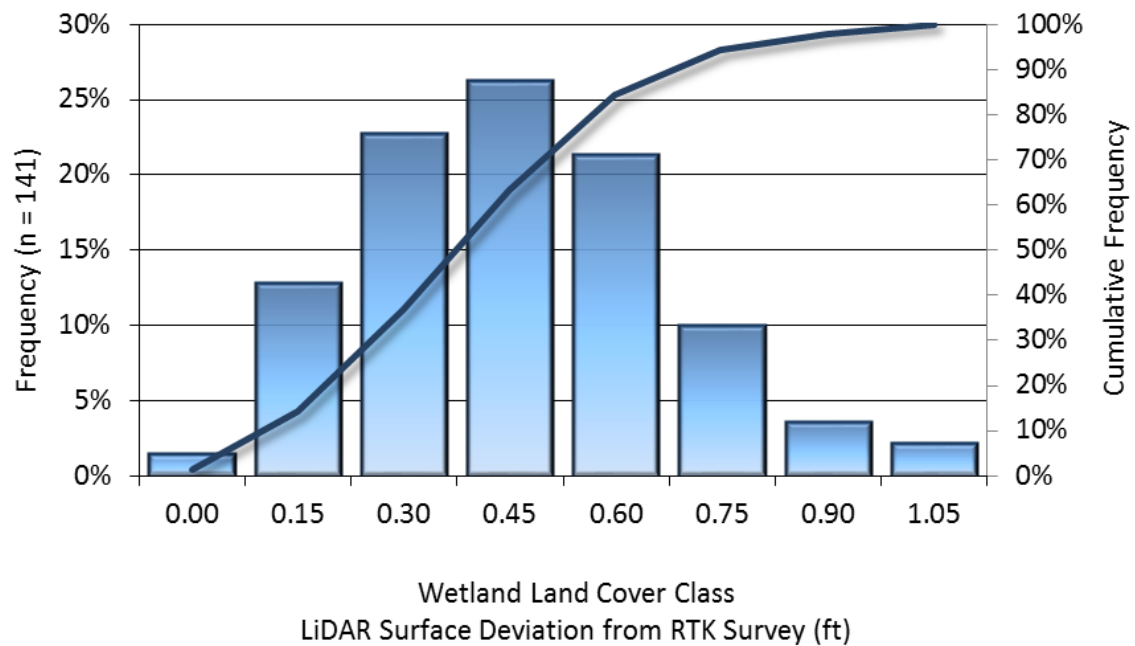
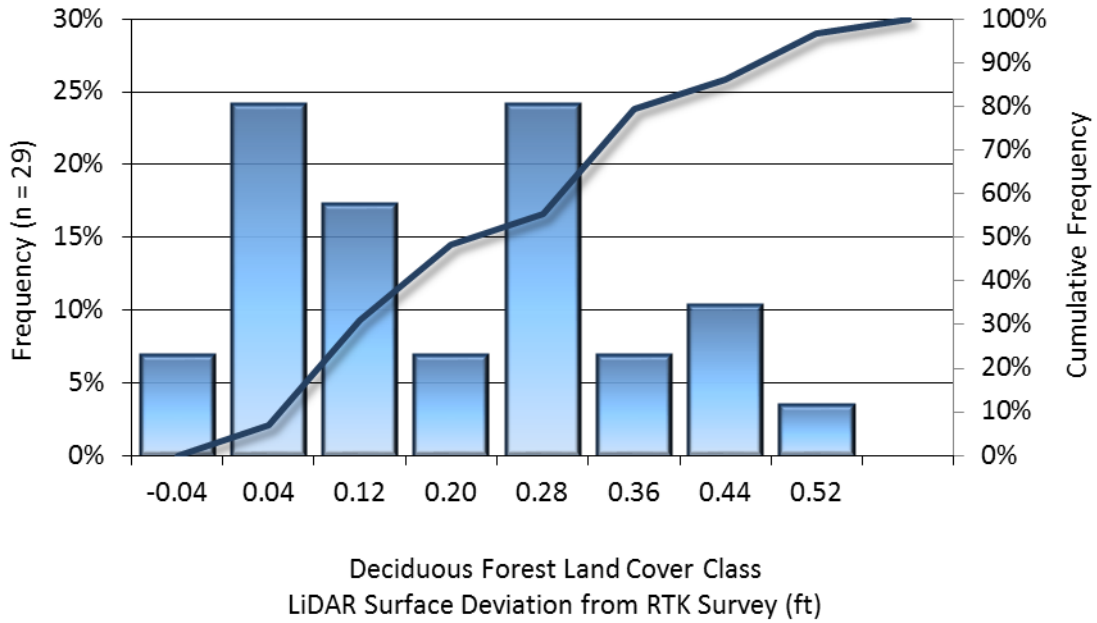
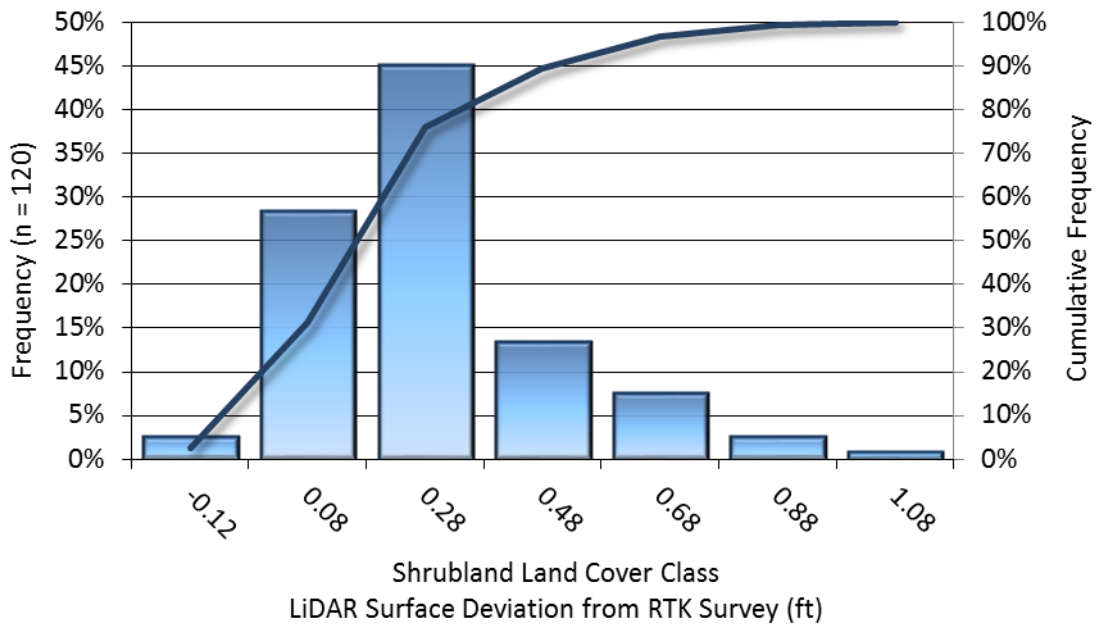


Figure 54: Frequency histogram for LiDAR surface deviation from Wetland Landclass RTK values



**Figure 55: Frequency histogram for LiDAR surface deviation from Deciduous Forest Landclass RTK values**



**Figure 56: Frequency histogram for LiDAR surface deviation from Shrubland Landclass RTK values**

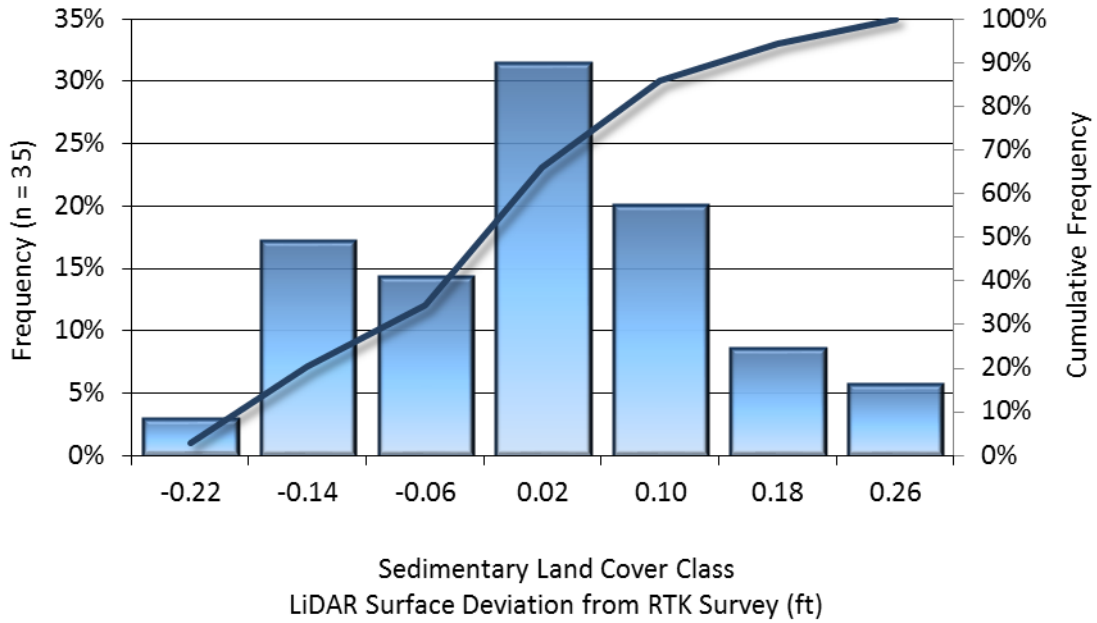


Figure 57: Frequency histogram for LiDAR surface deviation from Sedimentary Landclass RTK values

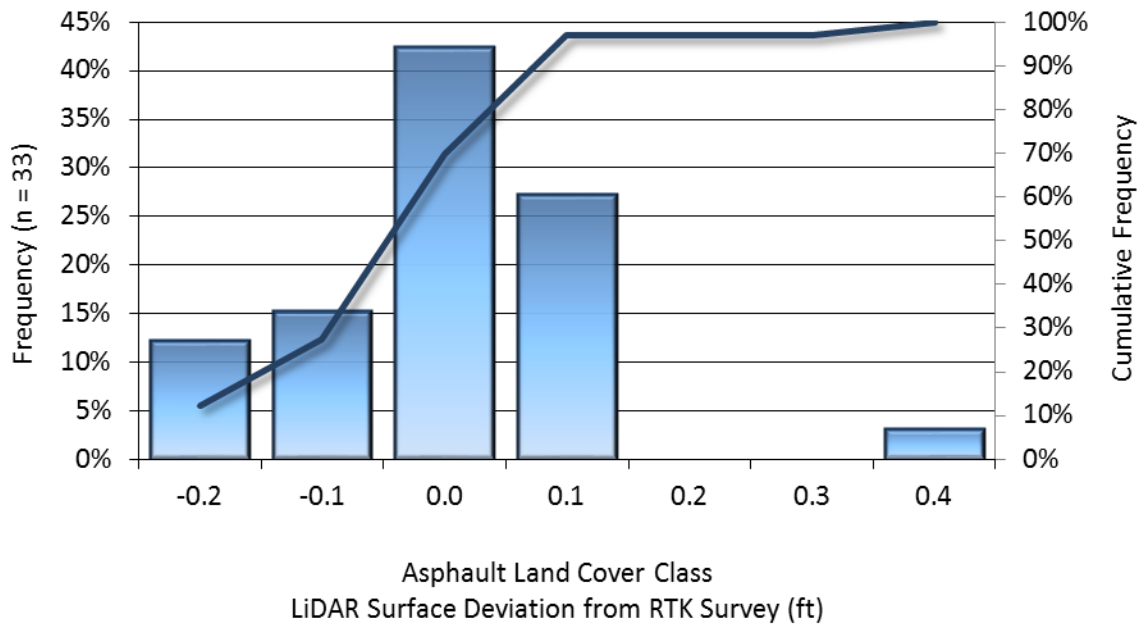
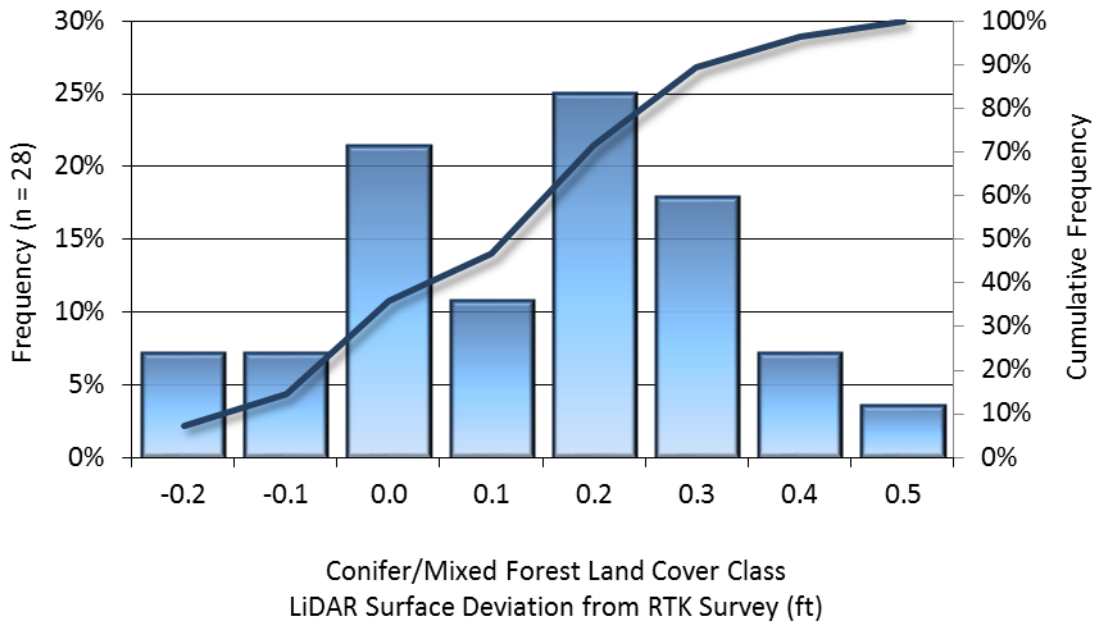


Figure 58: Frequency histogram for LiDAR surface deviation from Asphalt Landclass RTK values



**Figure 59: Frequency histogram for LiDAR surface deviation from Conifer/Mixed Forest Landclass RTK values**